THE SIMPLE MEASUREMENT OF RESIDUE CURVES AND THE ASSOCIATED VLE DATA FOR TERNARY LIQUID MIXTURES

Theodoros Chronis

A Dissertation submitted to the Faculty of Engineering, University of the Witwatersrand, Johannesburg, in fulfilment of the requirements for the degree of Master of Science in Engineering

Johannesburg, 1996

DECLARATION

I declare that this dissertation is my own, unaided work. It is being submitted for the Degree of Master of Science in Engineering in the University of the Witwatersrand, Johannesburg. It has not been submitted before for any degree or examination in any other university.

T. Chenis

3rd day of May 1996

ABSTRACT

An apparatus to measure residue curves and the associated VLE data was designed. The apparatus was required to measure this data quickly, easily, cheaply and reasonably accurately. The Acetone, Benzene and Chloroform and the Acetone, Methanol and Benzene ternary liquid systems were measured to test the accuracy of the apparatus. In both cases, the results obtained correlated reasonably well with those predicted by theory using published data.

Two candidate entrainers for the 1-Hexene and Methyl Ethyl Ketone azeotrope were evaluated using the equipment. It was found that low boiling Acetone is not a suitable entrainer for the given system whilst high boiling Butanol is.

The thermodynamic interaction parameters were all evaluated during the course of the analysis. These were then used to generate residue curves over the full composition space for the systems investigated.

ACKNOWLEDGEMENTS

I would like to thank the following people and institutions without whose support I would not have been able to complete this project and thesis:

My supervisors, Professor D. G. Glasser and Dr. D Hildebrandt, for giving me guidance and a lot of help.

My parents and my brother for standing behind me and helping me through those hard patches that are always encountered.

Meg for always being there.

My friends in the Chemical Engineering Department and the Wits Explorers without whom work, the conditions of work and leisure time would not have been as good as they were.

B. Chassoulas (Baz) who helped me a lot with the commissioning of my GC and the running of it.

I wish to acknowledge financial support from the following institutions:

Sasol, Foundation for Research and Development and the University of the Witwatersrand.

CONTENTS   PAGE

FIGURE   PAGE

TABLE   PAGE

SYMBOLS

a : Calibration constant for the area under the GC peak

A_i : Margules coefficient for component i

A_{ij} : Margules coefficient for interaction between components i and j

AntA : 1st Antoine coefficient for species i

AntB : 2nd Antoine coefficient for species i

AntC : 3rd Antoine coefficient for species i

AreaA : Area under a GC peak for component A

AreaB : Area under a GC peak for component B

AreaD : Area under a GC peak for component D

B_i : Margules coefficient for component i

c : Constants relating moles of A to the area under the GC peak

d : Calibration constant for the area under the GC peak

Err : Error function on experimental values

f_l : liquid fugacity

f_v : vapour fugacity

H : Molar liquid holdup in the still (mole)

h : height of packing (m)

MolA : Moles of component A

Mol%A : Mole percentage of A

P : System Pressure (Pa or mmHg)

$P_{v,i}$: Vapour Pressure of Pure Component i (Pa or mmHg)

r : reflux ratio

s : reboil ratio

T : Temperature (K or °C)

t : Time (s)

V : Vapour molar flowrate (mole/s)

x_i : liquid mole fraction for component i

y_i : vapour mole fraction for component i

$\bar{y}$: vector of liquid mole fraction

$\bar{x}$: vector of vapour mole fraction

ζ : scalar quantity related to time

Φ_i : fugacity coefficient of component i

γ_i : activity coefficient of component i

Λ_{ij} : Wilsons coefficient for interaction between components i and j

σ_{yi} : Expected Error of the vapour mole fraction of component i

σ_T : Expected Error of the Temperature (°C)

Chapter 1

Introduction

1.1 Residue Curves and Distillation Column Design

Separation of azeotropic mixtures using distillation is industrially important but problems occur when complex multicomponent systems are examined.

A frequently used method for the separation of azeotropic mixtures is that of azeotropic distillation. It is sometimes possible to separate certain azeotrope-forming mixtures by using a simple sequence of columns without introducing other species into the system. Generally, this is not the case and thus the addition of an entrainer species is required as well as a more complex process configuration with one or more recycles.

The role of the entrainer is to either change the relative volatilities of the feed liquids in such a way as to facilitate separation or to introduce a new extreme azeotrope that also allows separation.

The design of the separation sequence may be divided into various parts, the screening of entrainers, the conceptual design of the separation sequence, the detailed design of the columns and the optimisation of the whole system (Wahnschafft et al, 1992).

Traditional methods for the selection of entrainers, design and optimisation of the sequence rely on rigorous simulation models that are time consuming.

Various methods have been suggested to handle optimisation. Until recently, there were no simple methods available to easily determine candidate entrainers and the possible distillation sequences for multicomponent distillation. The method of Residue Curves has recently been developed for the above two problems. This method predicts possible   aration for given ternary mixtures using only the topology of the Residue Curve Map. This information is essential to minimise the time spent modelling the system.

By being able to determine feasible separations, various candidate entrainers may be rejected if they do not allow separation of the products. This is a very useful screening procedure. In addition, this method may also be extended to determine possible configurations as it predicts whether a given separation is possible and thus the choice of separation sequences is simplified.

In general, it is very easy to model a residue curve map for a specific ternary system as it only requires a knowledge of the VLE of the system. It is thus very quick and easy to use these maps in the design process of azeotropic distillation.

1.2 Aims and Objectives

Currently, there is no easy experimental method to measure residue curves experimentally. It is easy enough to obtain them using theory, but this requires a knowledge of the thermodynamic interactions in the system. The curves may also be predicted using a group contribution method but this is not always sufficiently accurate for highly complex systems. This knowledge is not always available or not accurate enough thus necessitating an experimental approach.

The aims and objectives for this investigation are as follows:

1. To design and commission an apparatus that is able to measure residue curves quickly, cheaply and reasonably accurately.

2. To use this apparatus to measure known azeotropic systems and compare the results to those reported in literature.

3. To determine a suitable entrainer for the 1-Hexene-Methyl Ethyl Ketone azeotropic system using the apparatus designed. This system was selected as it is industrially relevant for the purification of α-olefins.

Chapter 2

Literature Survey

2.1 Introduction

Distillation is one of the most widely used separation processes. As a result, it is worthwhile obtaining a good understanding with the aim of eventually optimising such processes.

Often, nonideal interactions occur between components in mixtures. This may result in an azeotrope being formed between the liquids. An azeotrope is defined as being the point at which the vapour composition is exactly equal to the liquid composition.

Consider the case where it is required to separate a binary mixture of liquids, that forms an azeotrope, into the pure components. Traditional distillation methods rely on there being a difference between the liquid and vapour compositions. As the azeotropic point is approached within the distillation column, the difference becomes smaller until it disappears at the azeotropic point. No further separation is thus possible using traditional distillation methods so an alternative method has to be utilised.

The usual method utilised is the introduction of an entrainer. An entrainer is a third component that is added to the binary mixture to allow circumvention of the binary azeotrope. This entrainer may act in various ways so as to allow the separation of the two

azeotropic components. Each action has a different method associated with it so as to allow the required separation. There are four basic alternatives for separation through distillation (Laroche, 1992a):

1. Homogenous Azeotropic Distillation, where the entrainer changes the relative volatility of the azeotropic components,
2. Heterogenous Azeotropic Distillation, where the entrainer changes the relative volatility of the azeotropic components and induces liquid-liquid immiscibility,
3. Reactive Distillation, where the entrainer reacts with one of the constituents,
4. Salted Distillation, where the entrainer dissociates ionically and thus changes the azeotropic composition.

For the purposes of this study, only homogenous azeotropic distillation will be considered.

Generally there are a number of problems associated with azeotropic distillation and its design. Two such pertinent problems are the choice of an entrainer and the column sequence to be used to perform a given separation. Due to the nonidealities of an azeotropic system there is currently no accepted method to answer either of these questions other than a rigorous 'trial and error' steady state simulation.

A new graphical technique, Residue Curve Maps (rcm), has recently been developed and utilised to help solve the above

problems. This is a very new field of research and thus the reader should take note that there are many conflicting ideas in the literature. An overview of the current understanding of this technique will be given in this chapter.

2.2 Simple Distillation

Consider a vessel containing a liquid mixture that is open to the atmosphere. These liquids will evaporate if the temperature in the vessel is increased above the bubble-point of the mixture. All the liquids will not evaporate at the same rate as different liquids have different volatilities. This means effectively that some liquids 'boil off' or evaporate more easily than others. Generally, it is the case that liquids that are more volatile will evaporate at lower temperatures than others.

Thus, in a mixture, the more volatile compounds will evaporate at a proportionately higher rate than the other less volatile liquids due to the higher vapour pressure of the more volatile components. This means that the liquid in the still will become depleted in the more volatile component with time. Another fact that should be borne in mind is that the temperature of the system must increase if the more volatile liquids evaporate. Thus, as a typical boiling process occurs, both the composition of the liquid residue as well as the temperature in the still will change with time. The composition will change in such a way that the residue becomes depleted in the more volatile component and the temperature will increase monotonically. Similarly, the composition of the vapour removed will also change

and will usually show an increase in the amount of less volatile compounds with time.

The liquid composition residue and the composition of the vapour being removed may be measured. For ternary mixtures, these compositions can be graphed on a ternary set of axes. It is found that the above two compositions change in such a way that they each form a curve. The curve for the residue compositions is known as a *residue curve* whilst the curve for the vapour compositions is known as a *distillate curve*. Formally, a residue curve may be defined as being the locus of the liquid composition remaining from a simple distillation process (Doherty, 1978a).
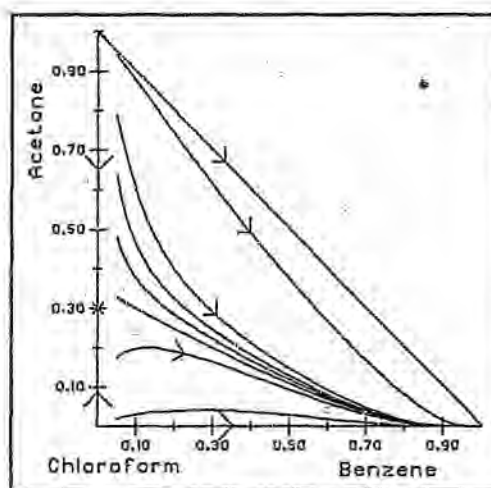
Figure 2.1. The Residue Curve Map for the Acetone, Benzene and Chloroform System

Different residue curves may be obtained by starting off with different compositions of liquids in the still. A set of these curves may then be plotted on a single set of ternary axes to give what is called a residue curve map. Generally, the y-axis represents the mole composition of the lowest boiling component and the x-axis that of the highest boiler. This convention will be followed throughout. A typical residue curve map, that of the acetone, chloroform and benzene system is shown in figure 2.1. Each residue curve has a direction associated with it and by convention it is indicated by arrows that indicate increasing time and thus increasing temperature. This is also illustrated in figure 2.1.

The topology of this map may be used to determine the viability of separating the three components in a sequence of distillation columns (discussed in section 2.8). In this way residue curves may be used to quickly and easily determine the suitability of potential entrainers for binary azeotropic systems. No reference was found in the literature to an apparatus that can be used to easily measure a set of residue curves has been designed.

The main aim of this dissertation is to design and test an apparatus for the measurement of residue curves and the associated distillate curves. Such an apparatus will thus generate the vapour liquid equilibrium data for the ternary systems under investigation. The apparatus and experimental method should be simple and inexpensive but such that the data is accurate enough to be used in the design of distillation columns.

2.2.1 Geometrical Considerations

There are certain rules that are obeyed in a ternary diagram. The lever rule is obeyed in the composition triangle. This means that if a mixture is split into two other mixtures of different compositions, all three compositions must lie on a straight line in the composition triangle. This line effectively represents a mass balance over any mixing or separation. This illustrated in figure 2.2. Material of composition M is split into two systems or streams of composition represented by points A and B respectively. The three points, A, B and M, all lie on the same straight line with the point M corresponding to the initial mixture lying between the points A and B.
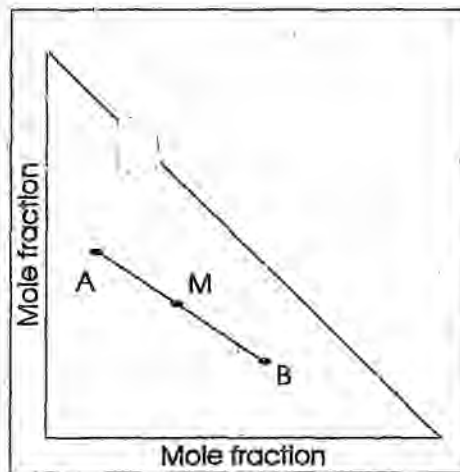
Figure 2.2. A Mass Balance in a Ternary System

This rule also applies to distillation columns. Consider a column with a feed indicated by point M. The tops and the bottoms from the column could be indicated by points A and B respectively. The

distance from A to M and B to M are in a ratio of the flows of the mixtures of composition B and A.

2.3 Residue Curves

The simple distillation system described in section 2.2 may be modelled mathematically. One of the assumptions of the above system is that the vapour that is produced will always be in thermodynamic equilibrium with the liquid which is the residue. Furthermore, the vapour is removed as soon as it is produced.
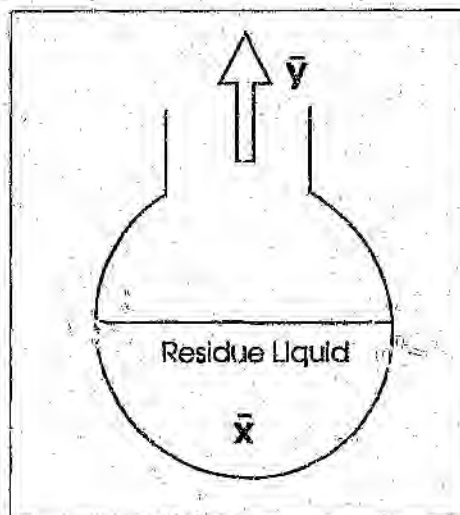
Figure 2.3. A Simple Distillation System

Consider the system shown in figure 2.3. This figure shows a typical simple distillation (boiling) system. The liquid residue is boiled in the vessel producing vapour that is in thermodynamic equilibrium with it. This vapour is removed as it is produced. An elementary

mass balance may be performed on the system shown in figure 2.3
to give equation 2.1 (Doherty, 1978a).

$$\frac{d\overline{x}}{d\zeta} = \overline{x} - \overline{y} \qquad (2.1)$$

$\overline{x}$ and $\overline{y}$ are the liquid and vapour compositions respectively and ξ is
a scalar quantity non-linearly related to time.

This equation relates how the composition of the residue liquid
and distillate changes with time and may be used to mathematically
obtain residue curves. The mass balance and derivation of equation
2.1 is shown in Appendix A. Doherty(1978a-b, 1979) does a full
derivation and analysis of this fundamental equation.

From the analysis by Doherty (1979a-b, 1979), residue curves
have the following properties:

1. The tangent to the residue curve at $\overline{x}$ and the vector
$(\overline{x}-\overline{y})$ are collinear,
2. Temperature increases monotonically with ξ along
the residue curve,
3. Singular points in the residue curve are either pure
components or azeotropes and are always isolated,
4. Residue curves cannot intersect in the interior or on the
boundary of the composition triangle. Convergence may occur

in a tangential manner,

5. The residue curve map may only contain nodes and saddle points.

2.3.1 Interpretation of Residue Curves

Equations 2.2 and 2.3 describe the composition profile in a packed column (Van Dongen and Doherty, 1985b) of distillate composition $\bar{y}_{i,D}$ and bottoms composition $\bar{x}_{i,B}$. Equation 2.2 describes the stripping section and equation 2.3 the rectifying section.

$$\frac{d\overline{x_i'}}{dh'} = \overline{x_i'} - \frac{r+1}{r}\,\overline{y_i} + \frac{1}{r}\,\overline{y_{i,D}} \qquad (2.2)$$

$$\frac{d\overline{x_i}}{dh} = \frac{s}{s+1}\,\overline{y_i} - \overline{x_i} + \frac{1}{s+1}\overline{x_{i,B}} \qquad (2.3)$$

where $\bar{x}$ and $\bar{y}$ refer to the liquid and vapour compositions respectively. $\bar{x}_{i,B}$ is the bottoms composition and $\bar{y}_{i,D}$ is the distillate composition, h is the height of the packing, s the reboil ratio and r the reflux ratio.

Consider the case when the reflux ratio and reboil ratios are infinite. In this case, both 1/s and 1/r are then equal to zero. Both

equations then simplify down to the residue curve equation. This indicates that residue curves correspond to the profiles in packed columns at infinite reflux and reboil.

At infinite reflux, it can be shown using the mass balance and the properties of residue curves, that: (a) the bottoms and distillate compositions must lie on the same residue curve and (b) the bottoms and distillate compositions and feeds must lie on a str   line (Laroche, 1992b). This is an important property in that it a   s for the design of distillation sequences for the limiting case of infinite reflux. The method in which this is done is explained further in section 2.8.

2.4 Azeotropes and Singularities

If one looks at equation 2.1, it can be seen that the left hand side of the equation will be equal to zero when the system has reached an azeotropic point or when the liquid is composed of only one component. In both cases, the vapour composition will be equal to that of the liquid. Any point at which this occurs is defined as being a singularity (Doherty, 1978a). In any given system there are a number of these singularities corresponding to azeotropes and pure liquids. The residue curves all begin and end at these singularities.

There are two types of singularities, namely node and saddle points. The starting and end points of residue curves are defined as being nodes and all other singularities are saddle points (Fien, 1994). Figure 2.4 shows an example of a saddle and a node point. A node

that is the origin of residue curves is unstable and that which is the end of residue curves is defined as being stable. In addition, one gets two different types of azeotrope. A low boiling azeotrope is one which has a lower boiling point than the pure components which make up the azeotrope while a high boiling azeotrope has a higher boiling point than those of the pure components. Generally, residue curves move towards higher boiling azeotropes or pure components and away from lower boiling azeotropes or pure components.
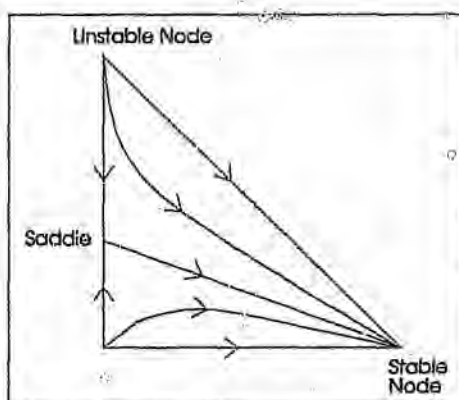
Figure 2.4. Two Different Types of Singularities

Foucher (1991) outlines a procedure for constructing the rcm for a system given all the necessary information (the singularities of the system).

2.5 Distillation Boundaries

Residue curve maps may be divided into distillation regions. Doherty (1978a) defines a distillation region as being a region in which residue curves start off close together and are still close together after some time. Figure 2.5 shows an example of a rcm with distinct distillation regions (a) while (b) has one distillation region.
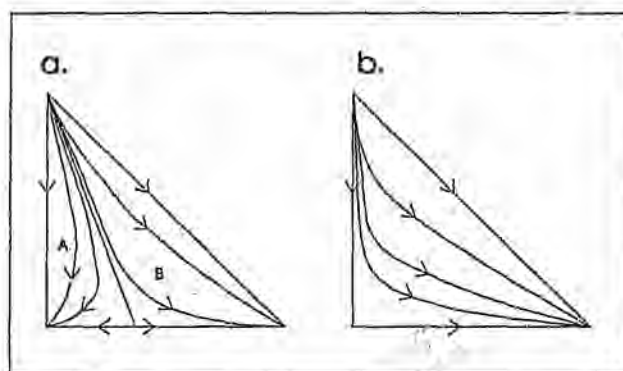
Figure 2.5. Residue Curve Maps with a) Two Distillation Regions and b) One Region

Distillation regions are bordered by distillation boundaries or separatrices. These separatrices are the residue curves which connect singularities. There are two types of separatrices, stable and unstable. Figure 2.6 shows an example of a rcm with a saddle. It can be seen that residue curves both converge and diverge from the separatrices. Those separatrices that have residue curves converging towards them are termed stable and the others are termed unstable. The unstable separatrices are those that are the distillation boundaries (Doherty, 1978a). The topology of a residue curve map for a specific

system must thus be known so as to be able to determine whether a given separatrix is unstable or not (Bossen, 1993).
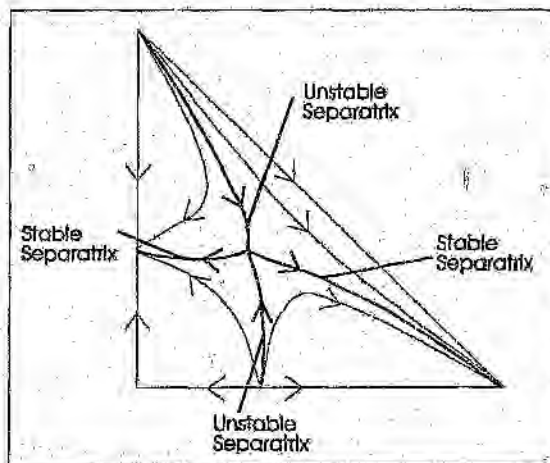
Figure 2.6. A Map with Stable and Unstable Separatrices

Rev (1992) defines a boundary as being the separatrix that arrives at a saddle point. Typically this is an unstable separatrix and agrees with the definition of Doherty (1978a).

There are many conflicting ideas as to the degree that the separatrices act as boundaries. Stichlmair (1989,1992), Doherty (1985) and Laroche (1992b) all put forward different ideas which will be discussed in section 2.6.

2.5.1 Distillation Boundaries and the Topology of Isotherms

The temperature always increases along a residue curve. As a result, there has been a misconception in the early literature that

ridges and valleys in the temperature contour plot act as distillation boundaries. This misconception was endorsed by Doherty(1978a) in his original article. Rev(1992) and Van Dongen (1984) acknowledge the fact that they do not form boundaries.

Rev(1992) gives a thorough discussion on this misconception and then goes on to disprove it. He shows that these ridges and valleys are not boundaries, through extensive modelling of various systems. An example of a boundary not coinciding with a ridge or valley occurs in the methanol, acetone and chloroform system.

Rev (1992) proves the above statements using the following argument. Consider a valley on the side of a hill. The bottom of the valley is descending monotonically. If one was to walk directly across the valley, one would have to first descend and then ascend to cross it. Now if one was to change your angle slightly, in the direction of the bottom of the valley, it would be possible to walk along the side of the valley whilst descending all the time, cross the bottom and then to walk out of the valley whilst still descending. This is possible as one would be basically following the bottom of the valley, diverging away from it slightly all the time. A valley could thus be crossed and therefore it is not be a distillation boundary. A similar argument may be followed for a ridge.

2.6 Effect of Distillation Boundaries

The residue curves correspond to packed column profiles at infinite reflux. These differ from a trayed column profile which is

described by difference equations and is thus stepped compared to the differential equations that describe residue curves and packed columns. A column profile is a plot of liquid compositions in a packed column. These column profiles still approximately follow residue curves at finite reflux. The distillation boundaries indicated by the residue curves may be shifted slightly by changing the reflux ratio. Wahnschafft (1992) shows where and how this shifting may have notable consequences on the shape of the boundary. These consequences are determined by simulating a packed column at various feeds and reflux ratios and thus determining the boundaries. It is generally found that the boundary indicated by the residue curve method has to be very curved for any effect to be apparent. Doherty (1978a) realises that the boundaries may be crossed at finite reflux, when very curved but surmises that the degree of crossing is very small, therefore not viable.

Consider the case where a given residue curve approaches a curved distillation boundary closely. If the residue curve approaches this boundary from its concave side, the associated distillate curve can lie in the other distillation region. In this way a border crossing is possible at finite reflux as the tops and bottoms points are not required to lie on the same residue curve. Figure 2.7 indicates how a vapour point from a distillation boundary lies in another region. The boundary cannot be crossed by an approach from the convex side as the distillate composition is in the same region. When the column is being run at infinite reflux, both the tops and the bottoms of the column must lie on the same residue curve. Residue curves may not intersect, which would be the only way the cross a boundary directly,

thus the boundary cannot be crossed at infinite reflux.
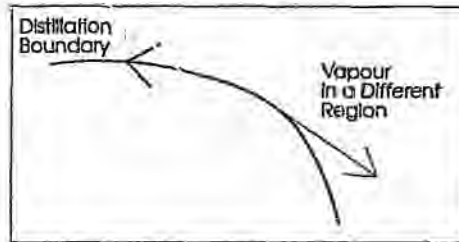
Figure 2.7. Border Crossing at Finite Reflux

·Consider the case of the boundary being a perfectly straight line. The distillate will lie on the boundary. As a result, the distillate cannot move the column into another region and thus the boundary cannot be\ crossed. This is the\only case when a boundary may not be crossed at all.

Another type of boundary crossing, possible at infinite reflux, is that obtained by mixing intermediate products to move feeds from one distillation region to another, thus facilitating boundary crossing. Doherty (1985) attempted to use this approach but was not able to succeed for mass balance reasons and the fact that the assumed boundary was a straight line. Stichlmair (1992) was able to perform this boundary crossing using a recycle. This fact is reported in Laroche (1992a). The curve crossing is facilitated through the use of a recycle from both the second and third columns, effectively two recycles, to get the feeds into regions of the rcm where the boundary may be crossed. In addition, Stichlmair (1992) uses the large curvature of the boundary to facilitate the crossing. Stichlmair (1989) says that a separation is feasible when distillation lines begin and end

at the products. Figure 2.8 shows this type of boundary crossing where the curvature of the boundary is used. Distillation lines interconnect liquid concentration points and are obtained as follows. The composition of a vapour in equilibrium with a starting liquid is established. This vapour is then completely condensed to give a liquid with a different composition to that of the equilibrium liquid. The composition of this condensate gives the next point on the distillate curve. This process is repeated to give a distillate curve with different curves resulting from different starting points. Distillation lines are similar to residue curves, thus if there is a curve that connects both the proposed products, the separation is possible. This is used for curve crossing only when the boundary is very curved as has been mentioned. The above curve crossing is possible though it is a complex system and thus difficult to design.

This type of curve crossing was also reported by Laroche (1992b). In this case, the feed is in a different region to that of the distillate and bottoms from the column. The curve crossing is shown in figure 2.8. The feed has to lie close to the concave side of the boundary. By the mass balance law, all three compositions must lie on the same straight line and the tops and bottoms from the column must be on the same curve for a column both,   at infinite reflux. It can be seen from the figure that the curve has been crossed due to the high curvature of the boundary. The design of a system with this type of crossing requires data that is highly accurate in that it depends on the shape of the boundary. The column also has to be run very stably to keep the feed in the right area of the residue curve map. Bossen (1993) highlights these two facts in saying that the

degree of curve crossing is determined by the shape of the boundary and the position of the feed. Furthermore, this system would be very expensive and difficult to control (Foucher et al 1991, Stichlmair and Herguijuela, 1992).
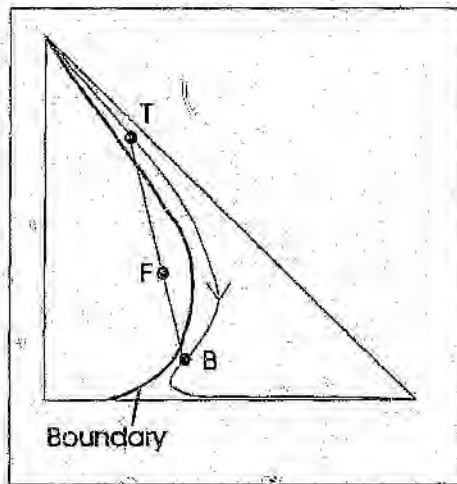
Figure 2.8. Boundary Curve Crossing

Finally, Wanschafft et al. (1992) say that "the extent of crossing of simple distillation boundaries will hardly ever be large enough to make species, which introduces such a boundary between the components to be separated, a good choice as an entrainer." This suggests that the choice of entrainer should be such that the required products are always in the same distillation region.

2.7 Possible Products from a Column

It may thus be assumed that for a good stable design of a distillation column, a distillation boundary may not be crossed by a single column even at finite reflux. It may be crossed by a column

sequence, though this fact is disputed by Doherty and Caldarola (1985).

The rcm may be used to determine what the possible tops and bottoms compositions are for a column with a specific feed. There is a 'shortcut' method that may be employed, the 'bowtie' method. This method specifies what possible top and bottom products may be obtained from a column for a specific feed. It relies on two important lines, the direct split and indirect split lines (Fien, 1994) shown in figure 2.9. The direct split is the line that connects feed composition and the lowest boiling vertex in a distillation region indicating a split with the lowest boiling species as a top product. The indirect split is the line connecting the feed to the highest boiling vertex in the distillation region, indicating a split with the highest boiling species as a bottoms product.
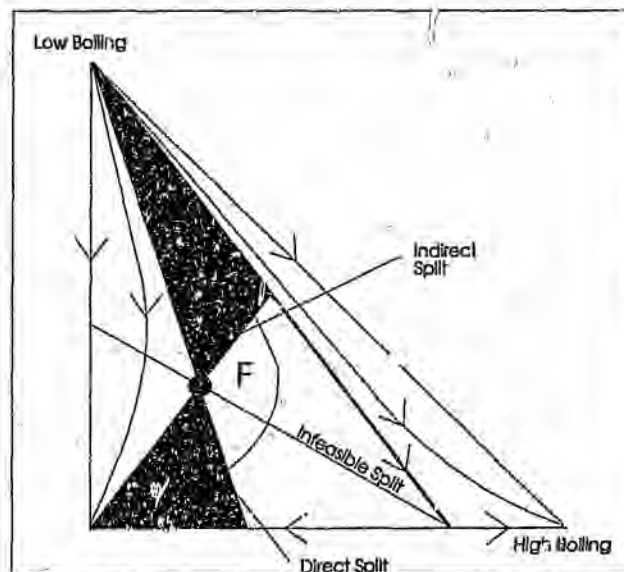
Figure 2.9. The Direct, Indirect and Impossible Splits

To obtain the bowtie regions, the indirect and direct split lines are drawn on the relevant residue curve (figure 2.9). These lines split the distillation region into four regions. It should be noted that the split lines are restricted by any distillation boundaries as the profile from a single column may not cross a boundary.

Examples of possible splits (the direct and indirect splits) and an impossible split are shown in figure 2.9. The one split is impossible as there is not a residue curve that is intersected twice by the mass balance. The two areas that this line goes through are therefore not possible products from a column and are thus discarded. The other areas are shaded to indicate that they are possible products from the column. Finally, a feasible residue curve must go through both shaded areas and also intersect twice with the mass balance line through the feed composition. Thus, the feasible region will lie on the convex side of the residue curve going through the feed as indicated in figure 2.10. The shaded region is the 'bowtie' region for a specific feed.
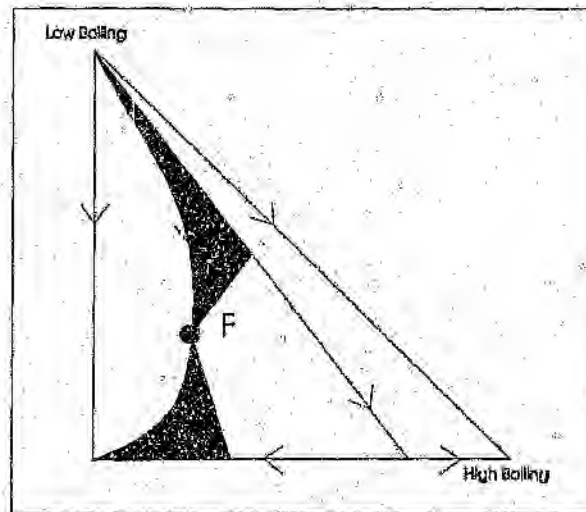
Figure 2.10. The 'Bow-Tie' Region

These regions may be generated mathematically as described by Wahnschafft (1992). The resulting regions are generally smaller than the real achievable regions but may be computed with sufficient accuracy for preliminary design procedures. Bowtie regions may be complicated if the feed lies near an inflection point in the residue curve and thus it may not be defined merely in terms of direct and indirect splits (Wahnschafft, 1992). Finally, it should be realised that the bowtie method is a shortcut method that may rule out feasible tops and bottoms products that are possible with finite reflux systems.

2.8 Column Sequencing

The usefulness of residue curve maps is that they allow the designer to easily determine a viable column sequence with no

simulation of the column being required. The method used relies on the fact that mass balances must always be obeyed and boundaries cannot be crossed directly by column profiles.

The first example is a straightforward non-azeotropic distillation. The rcm and associated column sequence is shown in figure 2.11. This example shows a direct split being used to split components A, B and C. In the first column, pure A is removed out the top and a mixture of B and C sent to the second column where they are separated. Other configurations that could be used are the indirect split and the nonsharp split. The indirect split relies on C being removed in the first column and the other two components being removed in the second. The non-sharp split would require three columns to achieve separation. As a result, one normally distils to a composition of interest (pure component or azeotrope) to minimise the number of columns required. Non-sharp splits may be used for heat integration, balancing molar flowrates to other columns or isolating difficult separations (Fien, 1994). Non-sharp columns are normally used as preconcentrators.
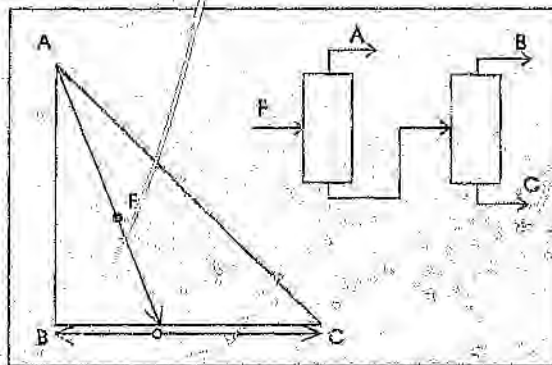
Figure 2.11. A Non-Azeotropic Separation

There was no azeotrope present in the above system. This gives the designer a lot of freedom in the choices that may be made with regards to column configurations. When azeotropes are present, the problem is more constrained in that a lot fewer options are available. Consider the following example that is taken from Stichlmair (1992).

The residue curve map for the system is shown in figure 2.12. The components a and b are the desired products with e being the entrainer. The column configuration and associated mass balances for this separation are shown in figure 2.13.
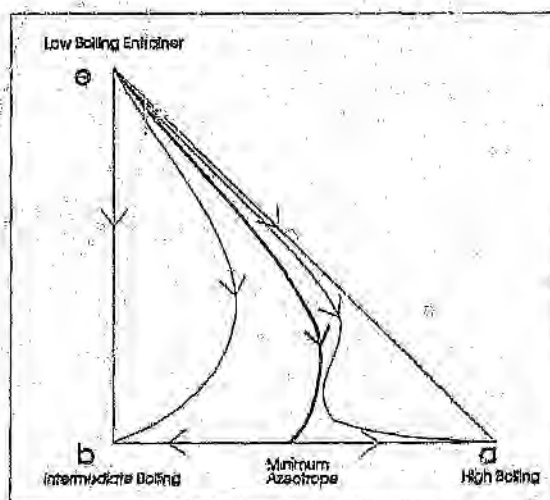
Figure 2.12. The Residue Curve for the System Under Question

The feed lies in the region where a can be obtained as a pure component. Stichlmair (1992) suggests that F be mixed with the yet unknown bottoms stream B3 to obtain the feed mixture M1. M1 is

then fed to column C-1 that has bottoms B1 and distillate D1. D1 is then mixed with the unknown D3 to give M2 which is fed into column C-2. The products from this column are B2 (the bottoms) and the distillate D2. D2 is then fed to column C-3 where it is split into the products D3 and B3 which are now known. It is always advisable to keep the recycle small for economic reasons. Thus, by the lever arm rule, the length B2-M2 must be much larger than the length D2-M2. This requires a highly curved distillation boundary (for the curve crossing) and an optimal position for M2. This example gives some idea of how a typical column sequence could be determined. It may be noted that there is no simulation required other than that for the residue curve, cutting down on a lot of time that would have otherwise been spent trying to determine a viable column sequence.

The above solution is very expensive in terms of capital and operating costs. It is a complex sequence with many columns and complications. therefore, wherever possible, the entrainer should be chosen so as to give a sequence with the minimum number of columns (2) and also as few recycles as possible.

Doherty and Caldarola (1985) give a good discussion on some of the possible pitfalls in column sequencing. An example they give involves an unspecified entrainer used for the separation of water and ethanol. The residue curve map is shown in figure 2.14 along with a suggested column sequence. The manner in which the separations and mixing occurs is self explanatory, following the same rules as used in the previous example.
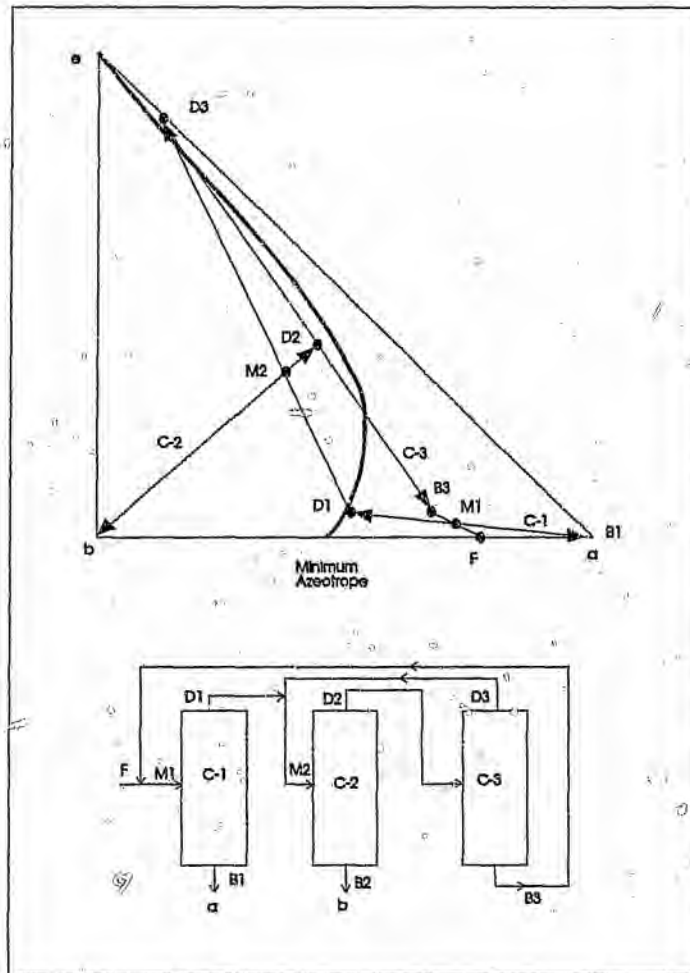
Figure 2.13. The Separation Sequence for the System Under Consideration
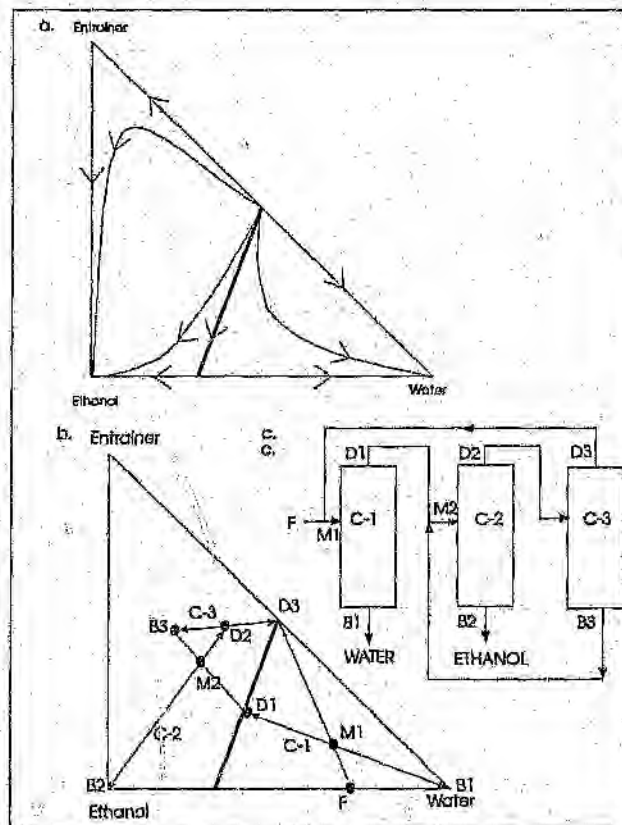
Figure 2.14. The rcm (a) and Suggested Separation (b,c)

Once the column sequence has been determined, it is normal to perform a simulation so as to ensure that the mass balance over the whole sequence converges. Doherty and Caldarola (1985) proceeded to do this and found that the system did not want to converge. They find that in order for there to be no mass accumulation in the system, all the water in F must be in B1 and all the ethanol must be in B2. If one looks at a mass balance over columns C-2 and C-3, it can be seen that D3, D1 and B2 must lie on

the same line. This requires that D1 be in distillation region II which is not possible to achieve with a simple distillation column. Doherty and Caldarola (1985) conclude from this and other case studies that "distillation boundaries within the composition triangle can never be crossed by simple recycle methods and that other sequencing techniques have to be employed". Laroche (1991) challenges this saying that the statement is only correct if the system is homogenous and the distillation boundaries are linear. From this it may be concluded that 'very' curved boundaries may be crossed or simple boundaries may be crossed using other methods such as decanting (heterogenous distillation) or reactions (reactive distillation). These examples show how important it is to keep the mass balances of the whole system in mind.

2.9 Alternative Separation Techniques

Homogenous distillation is not the only type of separation process available. Other processes are heterogenous, reactive and batch distillations.

Heterogenous distillation uses the fact that at certain concentrations, there will be two liquid phases of different composition present. These two liquid phases can be separated by decanting. In this way, it is possible to move across distillation boundaries. Residue curves may also be used for the design of this type of separation. Pham (1990a, b and c) gives a good introduction into the use of residue curve maps for the design of heterogenous distillations. Van Dongen (1983) presents a mathematical algorithm

by which it may be determined if a heterogenous system will occur in a specific ternary system.

In reactive distillation, the entrainer reacts reversibly with one of the constituents to be removed, thus allowing it to be removed by means of distillation. Barbosa (1988) and Venimadhavan (1994) show how this type of process may be modelled and residue curves used for the design of column sequences.

Van Dongen (1985a) shows how a batch distillation process may be modelled. He goes on to show how residue curve maps for batch distillations may be modelled and thus used for design.

2.10 General Rules for Selection of Entrainers

Various authors try and specify specific rules for the selection of entrainers. As is expected, they all have different rules and requirements from entrainers. Minimum-boiling azeotropes are normally considered as they are more common than maximum-boiling azeotropes (Laroche et al, 1992a).

Doherty and Caldarola (1985) consider all permutations of residue curve maps that contain at least one minimum-boiling binary azeotrope. They find that there are 87 different residue curve maps. Inherent in these maps are the assumptions that each side of the composition triangle can have at most one azeotrope and that there is a maximum of one ternary azeotrope. They attempt to use mixing to cross the separatrix but fail each time for mass balance reasons.

As a result, they conclude that the entrainer should be selected in such a way that it does not introduce a boundary between the components to be separated. Of the 85 rcm's considered, they find that 35 obey this condition. They therefore conclude that only entrainers that produced one of these rcm's should be considered for further design and optimisation.

Foucher, Doherty and Malone (1991) state that a sufficient condition for separability is that the components to be separated both lie in the same distillation region. This is the same condition that Doherty and Caldarola (1985) specified. Foucher *et al* (1991) present the seven most favourable maps for the separation of a low-boiling azeotrope. In their analysis they suggest that a straight line approximation of the separatrix is sufficient to determine separability. Finally, they present three different column sequences that may be used to achieve separation for the seven maps that they specify.

Stichlmair *et al* (1989) proposes a criterion that assumes the column profile cannot cross a distillation boundary. They specify the following rules for a minimum boiling azeotrope:

The entrainer must be a low-boiling substance itself or
The entrainer must form one or two new minimum-boiling azeotropes.

They present three feasible rcm's all with separatrices between the components to be separated as well as a three column sequence to perform the required separation. A set of rules for the separation

of a maximum-boiling azeotrope are also presented together with a column sequence for the separation.

Further rules for entrainer selection, distinguishing between processes with and without border crossing are developed by Stichlmair and Herguijuela (1992). Column profiles are once again assumed not to cross simple distillation boundaries but boundaries may be crossed by mixing of feasible products in systems with very curved boundaries. Processes that do not involve border crossings are developed using the criteria of Doherty and Caldarola (1985) that components to be separated must lie in the same distillation region. Stichlmair and Herguijuela (1992) present criteria that lead to processes with border crossings. Those for the separation of a minimum-boiling azeotrope are :

Low-boiling entrainer,

An intermediate entrainer that forms a new
minimum-boiling azeotrope with the lower boiling of the
other two components,

A high-boiling entrainer which forms low-boiling
azeotropes with both components, one of which must boil
at a lower temperature than that of the azeotrope to be
separated

The latter two rules are similar to those proposed by Stichlmair et al (1989). Once again, a similar set of rules is proposed for a maximum-boiling azeotrope. Various column sequences for the required separations are also presented.

Laroche *et al* (1992a) compares the rules presented by Doherty and Caldarola (1985) and Stichlmair *et al* (1989). He finds that the two sets of rules are contradictory. The rules of Doherty and Caldarola (1985) are termed "satisfactory" even though they reject many entrainers that would make separation possible. The rules by Stichlmair *et al* (1989) also reject candidate entrainers that make separations possible but accept entrainers that make separation infeasible. Laroche *et al* (1992a) analysed over 400 mixtures and their rcm's and determined the following classes of entrainer that always make a separation feasible :

Heavy (high-boiling) entrainers that do not introduce azeotropes,

Intermediate-boiling entrainers that do not introduce azeotropes,

The entrainer makes a separation feasible when the azeotrope is a saddle in the rcm. Light entrainers are also included in this category.

The authors also say that there are other classes of entrainers that make a given separation feasible but that they were not specified as the separation sequence could not be determined.

Laroche *et al* (1991) assesses candidate entrainers using equivolatility curves. These curves are used to split the composition triangle into regions, with the volatility order in each region being used to compare the various entrainers. Their method only considers entrainers that do not introduce azeotropes, comparing heavy entrainers with each other and light entrainers with each other. This

method may not be used for intermediate entrainers as the local volatility order has no meaning in the sense of ease of separability. Laroche et al (1991) justify this short coming claiming that the industrial use of intermediate entrainers is rare. Once the best heavy and light entrainers have been determined, the best of the two is determined by using a final cost for the proposed sequence.

Laroche et al (1992b) also developed rules for separability and column sequencing based on the convex hulls of the residue curves that go through t'   e required product compositions. This method applies only   lu   d as they admitted, it can exclude entrainers th   ie at finite reflux. An example of this type is that they ex   e   piling entrainers that are used industrially to separate minimum-   ..g azeotropes.

2.11 Further Factors Affecting Azeotropic Distillation Sequences

Partin (1993) says that ternary diagrams are a "powerful tool to present the compositions of three-component mixtures". As has been shown, residue curve maps are themselves a very powerful tool for the design of azeotropic distillation sequences.

Residue curves find their main application in finding feasible distillation sequences. Wahnschafft (1992) states that if a system is feasible at infinite reflux, it will be so at finite reflux as the infinite reflux system is an extreme case. It should be noted that the reverse is not true (Laroche, 1992b), as separation sometimes gets worse

with an increase in reflux ratio to the limit where the separation may not be possible at an infinite reflux but possible at a finite reflux.

In the previous discussion, nothing was said about the optimisation of a given system. This is a broad field that complements the residue curve theory. Knight (1989) presents a systematic optimisation algorithm. It relies on the minimum reflux being known after which a simple method of optimisation is followed. This minimum reflux may be obtained by the method described by Levy (1985). Knight (1989) finds that the most important optimisation variable is the ratio of the recycle to the feed (the feed ratio).

Another field of column design is that of choosing the conditions for the best heat integration. Knapp (1990) presents a method that uses a bifurcation and residue curve map analysis to thermally integrate columns. The bifurcation aspect is required as residue curve maps change their appearance at specific bifurcation pressures. This integration is performed once the sequence has been optimised as described by Knight (1989).

Finally, Bekiaris (1993) shows that certain distillation sequences can have more than one steady state. This is a fact that has to be taken into account in column design. They show that certain conditions in a residue curve map, such as two adjacent saddles, may lead to multiple steady states.

2.12 Concluding Remarks on Residue Curves and Azeotropic Distillation Sequences

Rcm's give a lot of information that may be used in the preliminary design of distillation columns and sequences. There is some disagreement in literature about the interpretation or behaviour of columns in certain situations.

We will later look at choosing entrainers that ensure that no boundaries need be crossed in the separation. The methods of Doherty and Caldarola (1985) and Laroche (1992b) appear useful as they allow us to find feasible entrainers for a specific separation even though they may reject many other feasible entrainers.

Measuring a rcm for a system that is not fully described will give many useful insights into the systems. It allows regions to be determined where the behaviour of the curves is critical eg. existence of boundaries, curvature and inflection points that are not obvious without the graphical representation.

Measuring rcm's allows one to :

1. measure VLE,
2. identify areas of potential interest as the rcm is measured allowing it to be examined more completely
3. obtain useful data for a new system.

2.13 A Brief Review of Various Vapour-Liquid Equilibrium Measuring Equipment

In practice there are two types of equilibrium cells that are used in vapour liquid equilibrium measurement. This classification is shown in figure 2.15 (Muhlbauer, 1990). The classification depends on whether liquid, vapour or both are circulated around the cell. If circulation occurs, the cell is classified as a dynamic cell and if not, it is termed a static. The basic principle behind each type of cell will be described.
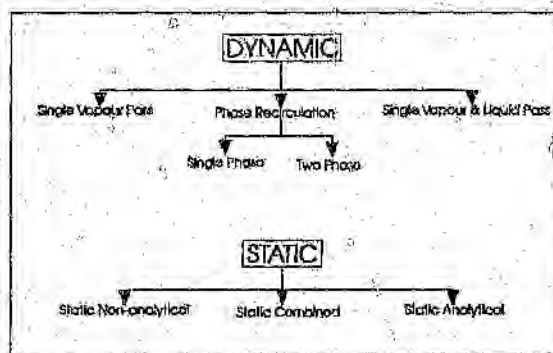
Figure 2.15. The Varieties of Equilibrium Cells

2.14 Static Vapour-Liquid Equilibrium Methods

The basic layout for this type of cell is shown in figure 2.16.
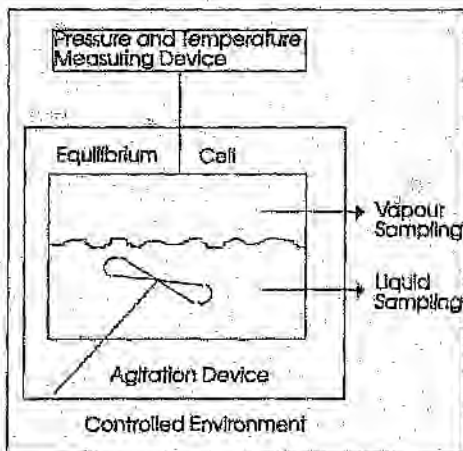
Figure 2.16. The Static VLE Apparatus

The mixture to be analysed is charged into the cell. This mixture is then agitated to promote contact between the phases, thus allowing an equilibrium to be established. Once equilibrium has been reached, samples of both the liquid and vapour are withdrawn and analysed using appropriate techniques. This sampling is done using different methods that are specifically designed not to disturb the equilibrium. The temperature and pressure of the system are also noted for modelling purposes. Once the necessary data has been obtained, a mixture of different composition is analysed. This procedure is followed until enough data has been collected. This method described is the static analytical method. In the non-analytical method, the phases are not analysed but the equilibrium is inferred from measured properties of the system and the initial starting compositions. This breakdown of methods is illustrated in figure 2.15.

Selected static Vapour-Liquid Equilibrium equipment is presented in Nakayama *et al* (1987), Ng and Robinson (1979), Guillevic *et al* (1983) and Kalra *et al* (1978).

2.15 Dynamic Vapour-Liquid Equilibrium Methods

Dynamic equilibrium apparatus can be classified into three categories : single vapour pass, phase recirculation and single vapour and liquid pass.

2.15.1 Single Vapour Pass Method

In this method, a pure gaseous component at a specific pressure is bubbled through a liquid phase in the equilibrium cell. The gaseous component progressively dissolves in the liquid until the vapour leaving the cell is in equilibrium with the liquid in the cell. The vapour and liquid may then be analysed. This method is presented in figure 2.17. An example of this method is presented by Young (1978).
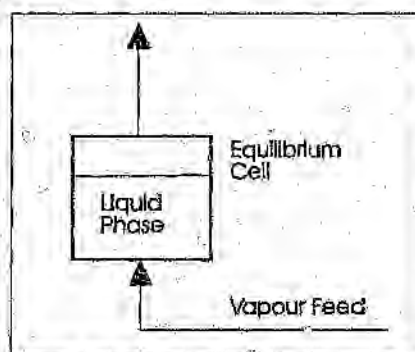
Figure 2.17. The Single Vapour Pass Equipment

2.15.2 Phase Recirculation Method

The components are charged into the equilibrium cell. Th temperature and pressure of the cell is maintained at the require levels while either one or both of the liquid and vapour phases continuously withdrawn from the cell and recirculated. In the metho where both phases are recirculated, the vapour and liquid phases a introduced countercurrently as is shown in figure 2.18. Once agai the two phases are sampled and analysed once equilibrium has bee reached.
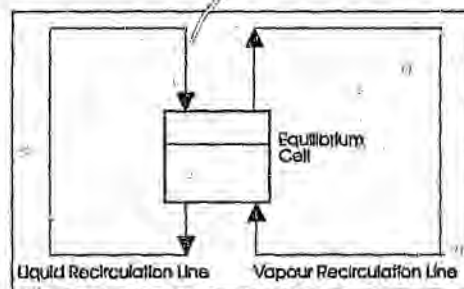
Figure 2.18. The Phase Recirculation Equipment Configuratio

This method allows the equilibrium to be established a l quicker than in the single pass method as the contact between th phases is much better. An example of this method is presented b Freitag and Robinson (1986).

2.15.3 The Single Vapour and Liquid Pass Method

Separate streams of vapour and liquid components are contacted cocurrently in a mixing unit that is maintained at a specific temperature and pressure. The combined stream is fed into the equilibrium cell where the two phases separate out and are removed separately. These two streams may be sampled. This method is shown in figure 2.19. Inomita *et al* (1986) presents a typical apparatus that utilises this method.
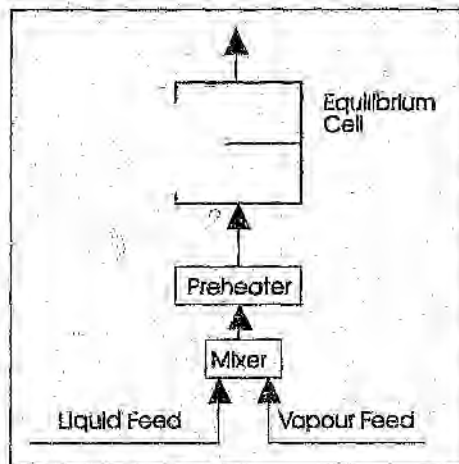
Figure 2.19. The Single Vapour and Liquid Pass Equipment Configuration

2.16 Concluding Remarks on Vapour-Liquid Equilibrium Equipment

Various methods for the measurement of Vapour-Liquid equilibrium have been presented. The final apparatus that will be presented for the measurement of residue curves uses a principle that

is similar to that of the single vapour pass apparatus as the vapour produced will only pass through the liquid once. It also allows a good contact between the vapour and liquid to give a reasonably good equilibrium.

Chapter 3

Theory and Calculational Procedure

3.1 Introduction

The models used to calculate the VLE data as well as the algorithm used will be presented in this chapter. This VLE data is required as it is the only way that may be used to determine how accurate and thermodynamically consistent the measured experimental data is. In addition, the algorithm which is used to fit models to the experimental data is presented.

3.2 Thermodynamic Models Used

Consider a two phase system. For the two phases to be in equilibrium, the fugacities of the phases have to be the same as is shown in equation 3.1.

$$f_v = f_l \qquad\qquad 3.1$$

where f_v is the vapour fugacity and f_l is the liquid fugacity.

The fugacity of the vapour phase may be written as shown in equation 3.2. If an assumption that the vapour phase is ideal is made, equation 3.2 may be simplified to give equation 3.3.

$$\hat{f}_v = P\, y_i\, \phi_i(P, T, y_i) \qquad\qquad 3.2$$

where P is the system pressure in Pascals, y_i is the molar fraction of component i, T is temperature in Kelvin and ϕ is the fugacity coefficient. For an ideal vapour phase, the fugacity coefficient is equal to one, therefore:

$$\hat{f}_v = P\, y_i \qquad\qquad 3.3$$

The fugacity of the liquid phase may be written as is shown in equation 3.4 with the assumptions that the vapour phase is a mixture of ideal gasses and that the liquid molar volume is negligible due to the low pressure.

$$f_i = x_i\, \gamma_i(x_i)\, P_{v,i}(T) \qquad\qquad 3.4$$

where x_i is the liquid molar fraction of component i, γ_i is the activity coefficient and $P_{v,i}$ is vapour pressure of component i.

Equating equations 3.3 and 3.4 gives equation 3.5 which describes how the vapour and liquid mole fractions are related to each other.

$$P\, y_i = x_i\, \gamma_i(x_i)\, P_{v,i}(T) \qquad\qquad 3.5$$

The systems that are investigated fall into two categories. The first is the category where the mixture is almost ideal. For this type of system, the Margules equation is used to determine the liquid activity coefficient.

The other type of system is that which is more non-ideal. Reid *et al* suggests that the Wilson correlation should be used to determine the liquid activity coefficient as it contains only two parameters and is mathematically simple to use.

The above two correlations for the liquid activity coefficients are used because they are both simple and easy to implement. They also give a reasonably good correlation with data provided they ε) used for the situations specified above.

3.2.1 The Antoine Equation

The vapour pressure for each component is determined using the Antoine equation shr wn in equation 3.6. The parameters for this equation are shown in Appendix B.

$$\ln P_v = AntA - \frac{AntB}{T + AntC}$$ 3.6

where P_v is the vapour pressure of the pure component in Pascal and T is in Kelvin.

3.2.2 The Margules Correlation

The Margules correlation for the activity coefficient is shown in equation 3.7 (Reid *et al*, 1987).

$$\ln \gamma_i = (1 - x_i)^2 \, [A_i + 2 \, x_i \, (B_i - A_i)] \qquad 3.7$$

where A_i and B_i are parameters.

This equation is only useful for a binary system but as ternary systems are being examined, the parameters in the correlation have to be adapted. They are adapted using equations 3.8 and 3.9. All the parameters used in equations 3.8 and 3.9 are those for the binary systems denoted by the subscripts. All parameters used in this equation are shown in Appendix B.

$$A_i = \sum_{j=1}^{N} \frac{x_j \, A_{ij}}{(1 - x_i)} \qquad 3.8$$

$$B_i = \sum_{j=1}^{N} \frac{x_j \, A_{ji}}{(1 - x_i)} \qquad 3.9$$

where $A_{kk} = 0$.

3.2.3 The Wilson Correlation

The Wilson correlation used to determine the activity coefficients for non-ideal systems is shown in equation 3.10 (Reid *et al*, 1987). The parameters used are shown in Appendix B.

$$\ln\gamma_i = -\ln\left(\sum_{j}^{N} x_j \, \Lambda_{ij}\right) + 1 - \sum_{k}^{N} \frac{x_k \, \Lambda_{ki}}{\sum_{j}^{N} x_j \, \Lambda_{kj}} \qquad 3.10$$

where Λ_{ii} is 1 and the rest are the Wilson coefficients given in Appendix B.

3.3 Simulation of Residue Curves

A residue curve map may be simulated if all the parameters mentioned in section 3.1 are known. A computer program written in turbo pascal that generates residue curves is presented in Appendix C. This program uses the equilibrium equations presented in section 3.2 together with a Runge Kutta routine to calculate the required residue curves.

3.3.1 Simulation Algorithm

Initially, the starting liquid compositions are specified in the program. From a specific liquid composition at i. bubble point, it is possible to determine the associated temperature. This is the case as the vapour mole fractions must all add up to unity. This fact is illustrated in equation 3.11.

The temperature is obtained by solving equation 3.11 for the one temperature that will make the right side of 3.11 equal to the total pressure of the system. Equation 3.11 was obtained by summing equation 3.5 for all i.

$$P = x_1 \; \gamma_1 \; P_{v,1} + x_2 \; \gamma_2 \; P_{v,2} + x_3 \; \gamma_3 \; P_{v,3} \qquad\qquad 3.11$$

Once the pressure is known, the vapour compositions may be calculated using equation 3.5. As a result, the right hand side of the differential equation describing residue curves (equation 2.1) is then known. The differential equation is then integrated using the Runge Kutta routine (Ralston and Rabinowitz, 1978) to give the next liquid composition on the residue curve from which the temperature and vapour compositions may once again be calculated.

The above procedure is repeated until the residue curve reaches a stationary point at which point the program is exited. The program may thus be used to calculate a series of residue curves so as to obtain a residue curve map.

The above algorithm may be adapted to calculate the predicted VLE for various starting liquid compositions so that experimental results may be compared with theory.

3.4 Analysis of Experimental VLE Data

The models described in the previous section were used to determine

the necessary parameters to describe a specific ternary system. These parameters are those needed in the Wilson and Margules models. The fitting of the models was achieved through the use of programs written in the Matlab package.

A schematic of the basic algorithm used is shown in figure 3.1. The Matlab programs used for both the Margules and Wilson correlations are shown in Appendix C.
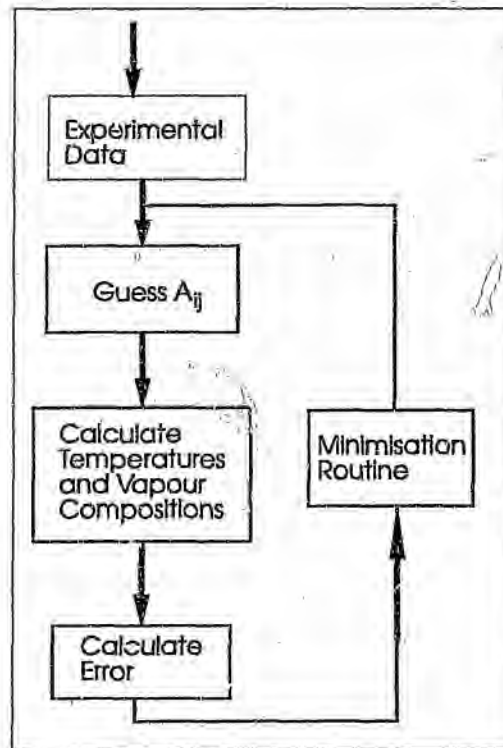
Figure 3.1. The Basic Model Fitting Algorithm

The models are fitted at each point to the experimental VLE data that is measured over a series of runs. The data recorded consists of the liquid compositions and the associated temperatures and vapour compositions.

Initially, the parameters for the specific model being fitted are guessed. These values are then used to calculate the temperatures and vapour compositions associated with a series of measured liquid compositions. Equation 3.11 is solved to give the temperature associated with a specific liquid composition. It is possible to solve this equation as the only unknown is that of the temperature. This equation is obtained by summing both sides of equation 3.5 and using the fact that the vapour compositions have to add upto 1. The *fmins* function is used in Matlab to determine the temperatures.

Once the temperatures have been determined, the vapour compositions may be determined using equation 3.5 together with the temperature determined in the previous step.

Once the vapour compositions and related temperatures have been determined, a residual which is the difference between the measured experimental value and that calculated using the model is calculated for each experimental VLE point. An error associated with each variable may then be defined as being the sum over all the VLE points of the squares of the residuals divided by the square of the expected error with the total error being the sum of all the individual errors. This error function is shown in equation 3.12.

$$Err = \sum \frac{(\Delta y_1)^2}{\sigma_{y_1}^2} + \sum \frac{(\Delta y_2)^2}{\sigma_{y_2}^2} + \sum \frac{(\Delta y_3)^2}{\sigma_{y_3}^2} + \sum \frac{(\Delta T)^2}{\sigma_T^2} \qquad 3.12$$

where Δy_i and ΔT are the residuals for the vapour composition and temperature and σy_i and σT are the expected errors.

The expected errors are approximated by comparing the measured results to those predicted by theory for both the vapour compositions and the temperatures.

The fmins function is used once again to minimise this error with the parameters in the activity coefficient model being the variables that the error function is being minimised with respect to.

The above method gives the coefficients for a specific activity coefficient model that is associated with measured data. It was realised that the error in the temperature measurement was much greater than that of the vapour measurement and thus only the vapour data was fitted to the models. The temperatures calculated were a hidden variable needed for the calculation of the vapour compositions in any case. In this way, the calculated vapour compositions took into account the calculated temperatures.

3.5 Concluding Remarks

The basic methodology behind the simulation of residue curves as well as the analysis of VLE data has been presented.

It may be suggested that the residue curve equation be used to analyse the experimental data and so obtain the necessary coefficients. It was decided not to follow this method as a small initial error in a composition would result in much larger errors occurring later in the algorithm. This is the due to the fact that a differential equation is being fitted. As a result, only individual VLE points are considered for the analysis. The parameters calculated will be used to simulate residue curves which will be compared to those experimentally measured.

Chapter 4

Experimental Method and Apparatus

4.1 Introduction

It has been shown that residue curves are very useful for the design of distillation column sequences. A simple apparatus for the experimental measurement of these curves is required in order to measure these curves for systems for which there is no experimental data available. Thus an apparatus is required that can be used to measure residue curves as well as the associated vapour compositions and temperatures.

These values have to be determined reasonably accurately with the method used also having to be quick, easy and simple. The challenge is thus to design an apparatus that balances ease of use and speed with accuracy.

The factor that has to be considered in the design of this apparatus is that the vapour leaving the still at a specific time has to be in thermodynamic equilibrium with the remaining liquid. Initially, it is not clear how easy this is to achieve. Similarly, the temperatures of both the vapour and liquid have to be the same but once again it is not obvious how easy this will be to achieve.

The philosophy used in the design of the apparatus will be that the apparatus must be kept as simple as possible keeping in mind that results of a high accuracy are not required. This is the case as the residue curves determined will probably only be used in the initial entrainer selection phase

and column sequencing and possibly not in the final design of the distillation columns. The end result was that a very simple apparatus was initially used with modifications being kept to an absolute minimum. Hence, two setups were finally investigated as will be explained further in this chapter.

4.2   General Description

The apparatus was designed so that residue curves could be measured during batch or simple boiling (ie. liquid compositions) as well as the associated temperatures and distillate curves (ie vapour) in equilibrium with the liquid residue.

There were various components to the experimental setup as shown in figure 4.1. The main component was the still. Two different designs of stills were used and the details will be described later in this chapter.
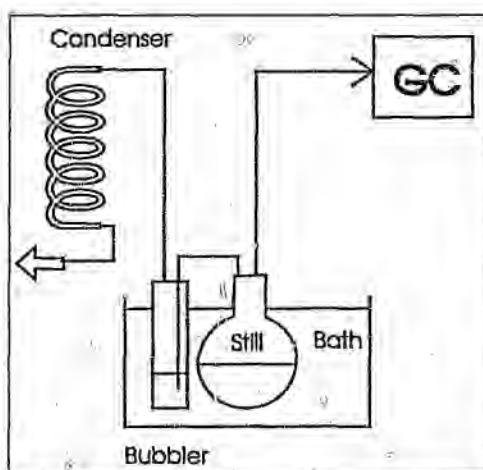
Figure 4.1. The Experimental Configuration

The still was kept in a Memmert oil bath. The purpose of the bath was twofold. The first was to ensure that the liquid residue would be at its bubble point. In addition, there was a temperature difference between the bath liquid and the residue that ensured that there was a net energy influx into the still. Obviously, the greater this temperature difference, the greater the rate of boiling. In this way, the boiling rate of the system was controlled by maintaining a specific temperature difference (the temperature of the bath being continuously increased).

There were temperature and liquid sampling ports on the stills. The temperature port allowed a pt-100 probe to be inserted into the still so that the temperature of the system could be measured. This probe works on the same principle as a thermocouple, but it has a reference link that corrects for errors that may occur as a result of long connections. The liquid port was covered with a septum so as to allow the sampling of the liquid using a needle without the introduction of air to the system that would disturb the equilibrium established.

The vapour produced in the still was removed using two spouts off the top of the still. The first spout is connected to the vapour sampling line that is connected to a gas chromatograph (GC). This GC with nitrogen gas as its carrier, was used for the analysis of mixtures that were sampled during the runs. The sampling in this line was done using a gas sampling valve. The second spout was used to control the pressure in the still by connecting it to a line that went through a bubbler and in turn a condenser. This pressure control will be discussed in more detail in section 4.5. The above two lines were both heated using heating tape to prevent condensation in them.

4.3   G.C. Running and Calibration

The analysis of the samples was performed with a 5860A Hewlett Packard gas chromatograph that had been recommissioned with new electronics. The column used was a Porapak Q column which is well suited for the analysis of light hydrocarbons. The signal from the G.C. was amplified using an inhouse amplifier and it was captured using an XT computer running on inhouse software.

The best operating conditions of the GC for each particular system had to be determined prior to any experimentation. The GC also had to be calibrated.

The operating conditions were determined by injecting a typical sample and seeing if the peaks separated out. If they ran into each other, the temperature of the oven was decreased and if they were too far from each other, this temperature was increased. The best operating temperature was chosen such that analysis of a sample would be as short as possible under the conditions while ensuring that the peaks were well separated.

Once a suitable operating temperature had been set, the GC was calibrated. Solutions of known composition were made and different quantities of these solutions were injected into the GC. The area under each peak was then measured. This area measured should be directly proportional to the moles of chemical that passes though the GC. This was found to be the case in that the constants derived were the same over a wide range of concentrations. This relation is shown in equation 4.1.

$$MolA = c \times AreaA \qquad 4.1$$

MolA refers to the number of moles of a component A, AreaA refers to the area under the GC trace for component A and c is the calibration constant.

There is a different proportionality constant for each chemical that passes through the detector. The areas that were measured for the calibrations may be used to determine this constant using equation 4.2.

$$Mol\%A = 100 \times \frac{a \times AreaA}{(a \times AreaA + AreaB + d \times AreaD)} \qquad 4.2$$

This is a simple equation that gives the mole fraction from known constants and Areas from a GC trace. Component B does not have a calibration constant as the constants for the other components are adjusted to make it 1. Using this equation, with known molar percentages and peak areas, the calibration constant a may be calculated and then used to calculate other molar composition with known GC peak areas.

A typical peak trace from the GC for the acetone, chloroform and benzene system is shown in figure 4.2.
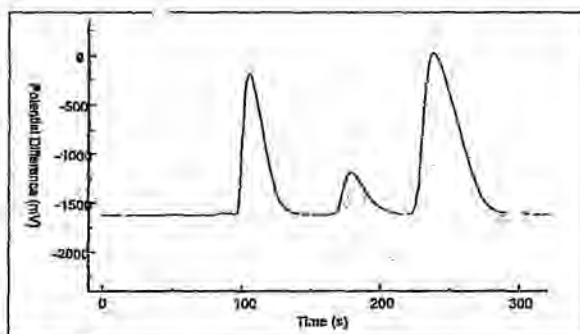
Figure 4.2. A GC trace for the Acetone, Benzene and Chloroform System

4.4   Vapour and Liquid Sampling

The vapour is drawn off through two ports, the sampling port and the pressure control port. The sampling port connects to a sample valve that in turn connects to the GC. The line that connects the port and the valve is heated using heating tape so as to prevent the condensation of the vapour. This is done as any condensation that may occur would influence the composition of the vapour going through to the sample valve and thus make these results invalid. The sample valve is also heated, for the above reason, using a heating cartridge that was mounted in an aluminium block.

The sample valve is a 6 Port External Volume Sample Injector. The valve circuit is shown in figure 4.3. In the valve's bypass position, the sample is flushed through the sample loop. The sample loop is a piece of stainless steel tubing with a volume of 1 ml. The vapour flushes through this loop and out through the waste port where it is collected. In the sampling position, the vapour bypasses this loop and goes straight out

through the waste port. During this time, the carrier gas flushes through the sample loop, flushing out all the vapour that was previously trapped in there.
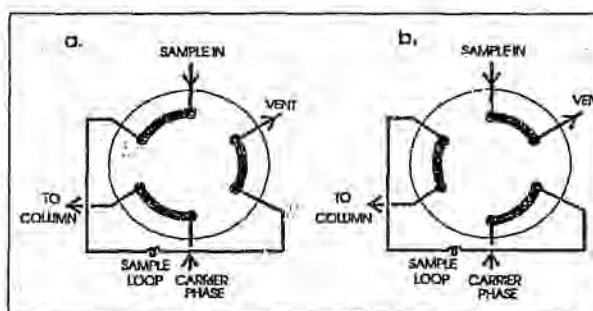
Figure 4.3. The Sampling Valve with the Valve in a. the Sample Mode and b. the Bypass Mode

The valve is turned using an actuator connected to a timer. The timer was set in such a way that the time it takes for the valve to return to its original position is the time the GC requires to analyse both a liquid and vapour sample.

The liquid sample was removed at the same time as the vapour sample. This was performed using a syringe with a 30cm needle. The liquid sample was injected into the GC using a 1 µl Dynatech syringe. The liquid sample was injected into the GC just after the vapour sample so that the liquid trace would appear just after that of the vapour sample. This was done so as to save time. The liquid was stored in ice prior to it being injected into the GC so as to prevent any volatiles from evaporating and thus causing the composition of the liquid sample to change.

4.5   Pressure Control

It was found that when the system was setup with only one port for gas sampling and no pressure control, the pressure in the system would rise as the pressure drop through the sample valve was too great. This was undesirable as the modelling would be complicated and the time taken for equilibrium to be reached would he much longer. Thus, a pressure relief line was put in. It is basically a heated line that goes from the still to a bubbler. This bubbler is kept in the water bath and is thus heated to the temperature of the bath.

Part of the vapour leaves the still down the pressure line and bubbles through water in a bubbler whilst the rest goes to the sample valve. The vapour passing through the bubbler does not condense as the water in the bubbler is hot enough to prevent this. The vapour from this bubbler then goes through a condenser where it is cooled and condensed using cold water.

The pressure in the still can be controlled by varying the oil level in the bubbler. It follows that if the oil level stays constant, the pressure in the still will also remain constant. This solves the problem of a changing pressure in the system when there was only the sample line. This is a simple yet very effective method used for the control of pressure.

4.6   Superheating and Nucleation Sites

Vapour formation occurs at nucleation sites during the process of boiling. If these sites were not there, vapour bubbles might not form, thus the liquid would start to superheat and flash directly to vapour. The vapour that is produced in this way is in equilibrium with the liquid at a superheated temperature. This temperature and vapour composition is not at the bubble point temperature for the specific liquid composition in the still. In the experimentation described, this is highly undesirable as the system would not be at its bubble point as required. As a result, nucleation points consisting mainly of pieces of stainless steel are used. It was found that these supplied sufficient nucleation points.

The ground glass joint was sealed using a teflon seal. This was done as the chemicals used in the systems measured dissolved vacuum grease. When this grease dissolved, it entered the still and coated the nucleation points, which did not work anymore and thus superheating occurred.

Superheating of the system also occurs when the heating rate of the waterbath is too high. This is controlled by keeping a very small temperature gradient between the liquid in the still and the bath. A typical difference is approximately 5 °C.

4.7   Initial Apparatus

The initial apparatus was kept as simple as possible in keeping with the philosophy discussed in the introduction.

The initial still was a 1l round bottomed flask with three spouts, for liquid and vapour sampling, and temperature measurement. This still was found to give reasonable residue curves whilst the VLE and temperature results were not as satisfactory. This is shown in the next section and the sources of inaccuracy are also discussed.

4.8   Preliminary Results

Initial results were obtained for the acetone, chloroform and benzene system using the above 'simple' apparatus. These results are shown in figure 4.4. The Residue Curve Map generated using the computer program described in chapter 3 are superimposed on the results shown in figure 4.4. It may be seen that there is some correlation between the results and the predicted curves but that this correlation is not all that good. Both the vapour compositions measured and the temperatures measured are not close enough to the values predicted by theory, even though the measured residue curves are reasonably close to those predicted by theory. It was proposed that this was due to the fact that the vapour evolved was not in contact with the liquid mixture for long enough and thus the vapour was not at the bubble point of the bulk liquid. This resulted in the inaccurate results. A new apparatus described later in this chapter was then designed to allow a longer contact between the liquid and vapour phases.
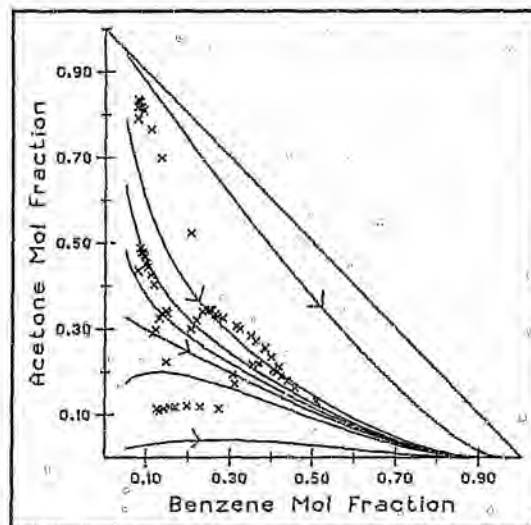
Figure 4.4. The Measured Residue Curve Using the Initial Apparatus

4.9   New Apparatus

The apparatus designed to facilitate greater contact between the two phases is shown in a schematic form in figure 4.5. The greater contact between the two phases is achieved by allowing the vapour produced to entrain some of the liquid as it rises.
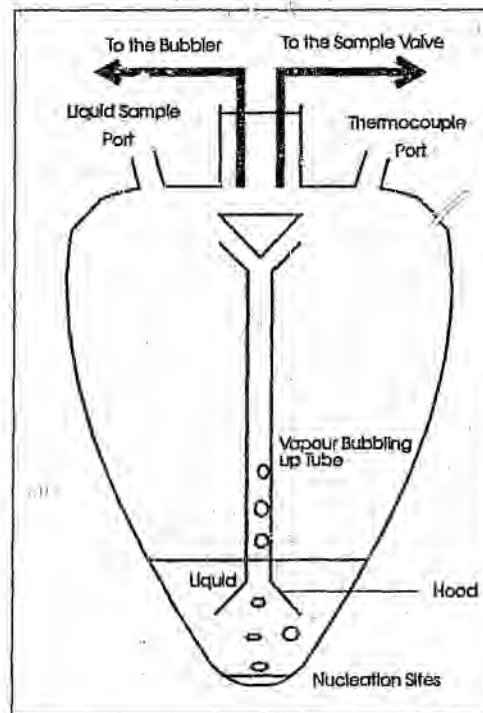
Figure 4.5. A Schematic Drawing of the Liquid Entraining Still

The majority of the vapour that is produced is captured by the hood that is in the liquid. This hood has a diameter of 3cm. This hood leads to a 6mm glass tube that leads to the top of the apparatus. The vapour goes up this tube, entraining some of the liquid, allowing the greater contact time. In practice the amount of liquid entrained is not very much but it has been found to be enough for a close approach to equilibrium to be achieved.

The tube that leads up, then flares into a funnel. There is a large conical piece of glass over this funnel. This glass causes the vapour that comes up the tube to be directed outwards, away from the sampling points. Any liquid that was entrained with the vapour is thus given time to separate

from the vapour before the vapour is removed from the system. This is required as even the smallest amount of liquid in the vapour sample will prejudice the accuracy of the results dramatically. In addition, this apparatus has a large space above the liquid. This also allows any liquid that may get splashed up in the process of boiling to separate from the vapour and drop back into the residue. Almost the whole still was immersed in the bath, thus exposing a small surface area through which heat losses could occur. This resulted in almost no partial condensation occurring that could affect the accuracy of the results.

The two gas sampling points are directly above the glass barrier. One point leads to the bubbler and the other to the GC.

A further feature of this apparatus is its shape. A conical shape was opted for as it allows a greater depth of liquid for a specific volume. This has the effect that the vapour once again stays in contact with the liquid for longer than if the apparatus was spherical. In addition, liquid sampling can be performed on smaller volumes of liquid. This is important as the depth of the liquid becomes a limiting factor for boiling and liquid sampling as the volume of liquid remaining becomes smaller.

The liquid sampling occurs through the port shown in figure 4.5. This port has a septum on it to ensure that all the vapour goes through the sample lines and that no air is introduced into the system. The sampling is done using a syringe with a long needle that is put through the septum and into the liquid. The temperature measurement is also done through a similar port. In this case a PT-100 probe is used. It is also inserted into the liquid through a septum.

A Residue Curve Map that was measured using the apparatus described is shown in figure 4.6. Once again, the theoretical curves are superimposed. The fit in this case is a lot better than that of the initial apparatus. In addition, the measured temperatures and vapour compositions are very close to those predicted using the theory.

Two different sizes of still of the same design were then compared. The dimensions of these two stills are shown in Appendix D.
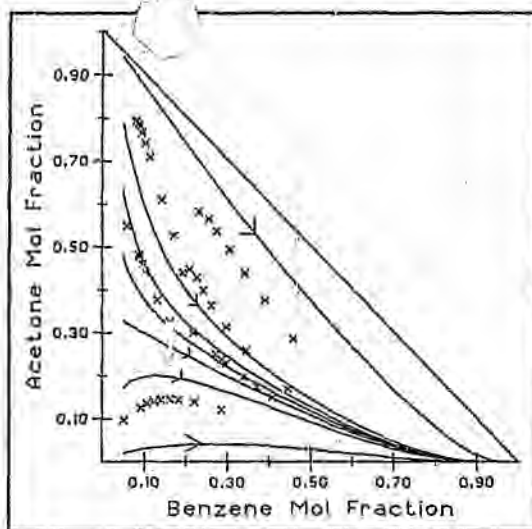
Figure 4.6. The Residue Curve Map Measured with the New Apparatus

A typical result for the acetone, chloroform and benzene system is shown in figure 4.7. The one line is for the large still and the second is for the smaller still. It may be seen that these results correlate well with each other and are thus reproducible within the expected accuracy of the apparatus. Due to the smaller still requiring less liquid it was used for the

duration of the project.
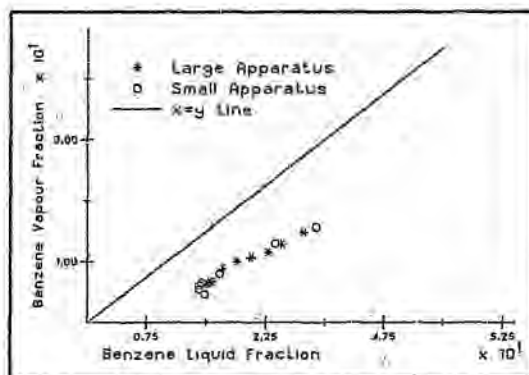
Figure 4.7. A Comparison of the Two Sizes of Apparatus in the Chloroform and Benzene Binary System

In the above experiments, both the calculated temperatures and vapour compositions were determined for each liquid composition. It was found that they correlated well with those measured using the new apparatus. The temperatures were within 0.2 °C and the vapour compositions were within 2 mol% of the predicted theoretical values.

4.10   Experimental Method

Initially, the liquid mixture is mixed and poured into the still. The temperature in the bath is then slowly increased until the liquid starts to boil. This is done by increasing the temperature of the bath so that it is always 5°C greater than that in the still. This has to be done otherwise the liquid in the still superheats.

Once the liquid is boiling, the sampling sequence is initiated. A liquid

sample is drawn at the same time as the vapour sample. The samples are then analysed as was described in section 4.3.

The next sample is taken once the analysis of the current sample has been completed. The analysis time for a vapour liquid pair varied from minutes for the Acetone, Chloroform and Benzene System to 17 minutes for the more complex 1-Hexene, Methyl Ethyl Ketone and Butanol System.

This process is continued until the level of liquid in the still is below that of the hood at which point the experimental run is aborted. This is necessary as the vapour evolved at this point is not present in sufficient quantities to displace any previous vapour evolved, thus vapour results may be inaccurate at this level of liquid. The liquid-vapour contact is also not good, thus possibly giving inaccurate results. At this point, the residue left in the still was approximately 20% of the initial charge.

4.11 Conclusions

The final apparatus used to measure Residue Curve Maps has been presented together with the experimental method to be followed. Preliminary results for the Acetone, Benzene and Chloroform system have been presented. They agree well with those predicted by theory, indicating that the apparatus is sufficiently accurate for the measurement of Residue Curve Maps.

Chapter 5

Results and Discussion

5.1 Introduction

Initially, the accuracy of the apparatus described in chapter 4 was tested using simple systems that have been well studied. The first was the acetone, benzene and chloroform system. This is a simple system that has an azeotrope in the acetone and chloroform binary. The boiling points of the pure components are shown in table 5.1.

The acetone, methanol and chloroform system was then studied. This was chosen as it produces a complex residue curve map with a ternary azeotrope and two binary azeotropes. The boiling points of the pure components are shown in table 5.1.

The two systems already mentioned were used to test the accuracy of the apparatus. This accuracy was found to be sufficient for the purpose of obtaining residue curve maps.

An entrainer to break the azeotrope between 1-hexene and methyl ethyl ketone was then sought. This system was chosen as no data could be found on the binary system but it could be predicted by the UNIFAC method. It was only known that an azeotrope is present.

Two candidate entrainers were initially selected. One was the lower boiling acetone and the other was higher boiling butanol. The boiling points of all the components of these systems are also shown in table 5.1.

Component	Boiling Point (°C)
Acetone	56.5
Benzene	80.1
Chloroform	61.2
Methanol	64.7
1-Hexene	63.3
Methyl Ethyl Ketone	79.6
Butanol	99.5

Table 5.1. The Pure Component Boiling Points at Atmospheric Pressure

All the binary systems measured were modelled as is explained in Chapter 3. The expected errors used in equation 3.12 were 0.02 (mole fraction) for the vapour compositions and 2 °C for the temperatures. The large temperature variance was chosen as there was a degree of superheating in the experimental system and thus

the measured temperatures would always be slightly different from the equilibrium temperature with the vapour compositions probably being more accurate. The standard deviations of the experimental data from the values predicted by both the literature and fitted parameters are quoted throughout. These standard deviations were obtained by applying the standard deviation equation to the VLE points.

5.2 The Acetone, Benzene and Chloroform System

Initially, residue curves for the various binary systems in this ternary system were measured. The results are given in Appendix E. The vapour-liquid diagrams are shown in figures 5.1, 5.2 and 5.3. The experimental values were analysed as is described in chapter 3. The Margules parameters thus obtained are shown in table 5.2 together with published values (Sandler, 1989). These parameters and the parameters quoted in literature were used to draw the theoretical and experimental curves shown in the figures.

Margules Parameters	Fitted Values	Lit. Values
A_{12}	0.00513	0.41022
A_{13}	-0.8871	-0.69344
A_{21}	0.4302	0.38501
A_{23}	-0.1801	-0.21715
A_{31}	-0.8400	-0.58056
A_{32}	-0.1803	-0.20229

where: Acetone : 1

Benzene : 2

Chloroform : 3

Table 5.2. The Fitted and Literature Margules Parameters for the Acetone, Benzene and Chloroform System
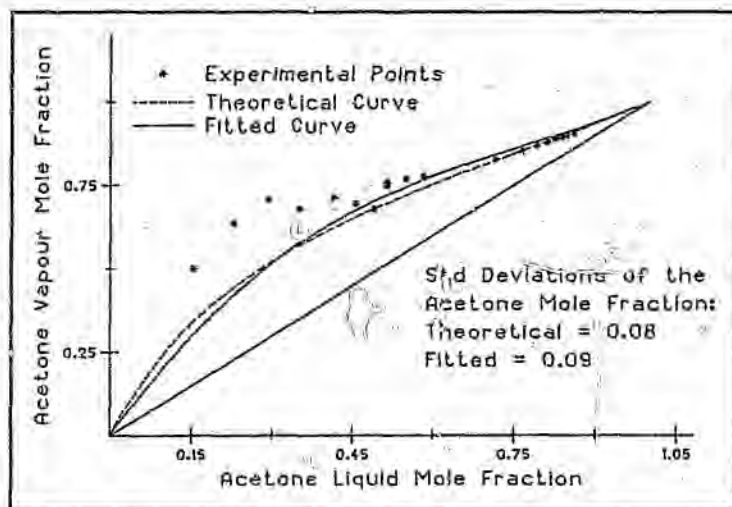
Figure 5.1. The Acetone Benzene Liquid Vapour Plot (83.6kPa)
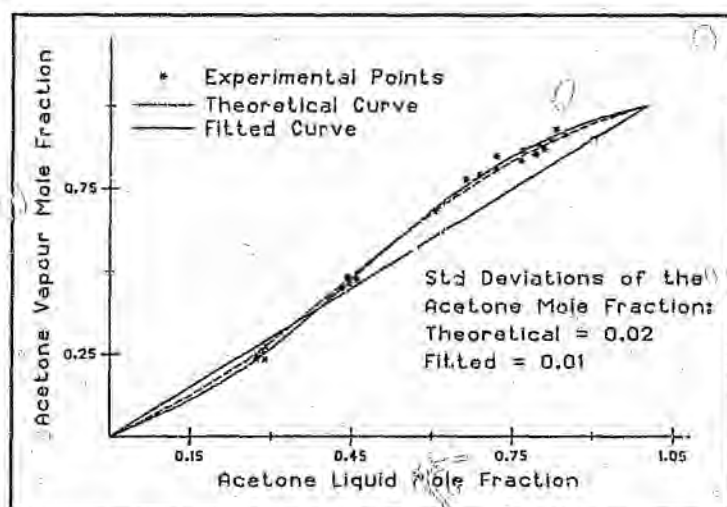
Figure 5.2 The Acetone Chloroform Liquid Vapour Plot (83.6kPa)
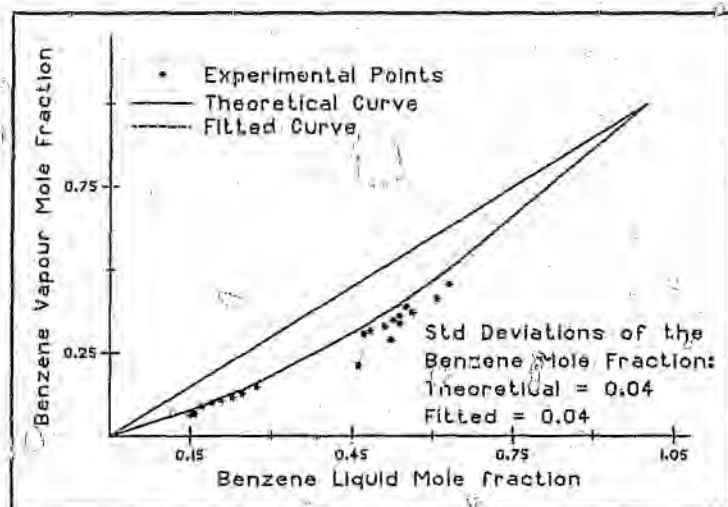
Figure 5.3 The Benzene Chloroform Liquid Vapour Plot (83.6kPa)

Generally, the vapour liquid curves correspond well to the measured data for both the literature and fitted Margules parameters. In addition, the two curves in all three binary systems correspond

reasonably well to each other indicating that the apparatus gives reasonably good liquid-vapour data. Interesting to note is that the fitted and predicted curves correspond exactly thus only one curve is shown. Furthermore, all data shown was used in the regression to obtain the thermodynamic interaction parameters. This data included both the temperatures and compositions with the compositions being weighted a hundred fold more than the temperatures.

The residual temperature diagrams for the above binary systems are shown in figures 5.4, 5.5 and 5.6. The temperature difference is the difference between the measured and calculated temperatures. In the acetone-benzene and benzene-chloroform systems, the temperature differences are all less than 2 °C. This is an acceptable value for the apparatus as a degree of superheating is expected. In the case of the acetone-chloroform system, the temperatures are up to 5 °C greater than those of the equilibrium temperature. This probably occurred as the heating rate for this system was higher than that for the other two binary systems, resulting in superheating. As a result, in future experiments the heating rate was set in such a way that the maximum temperature difference between the bath and the still was 5 °C. It is interesting to note that despite this superheating, the vapour liquid curve still corresponds well to the predicted values, indicating that the vapour composition can be measured accurately.
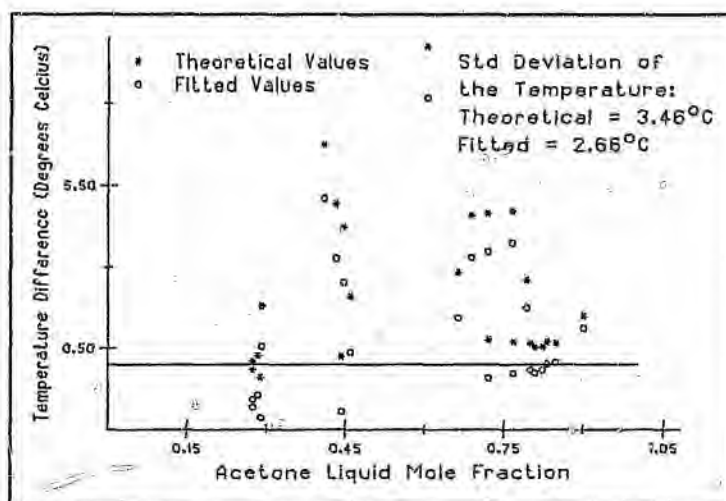
Figure 5.4 The Residual Temperature Plot for the Acetone Chloroform System
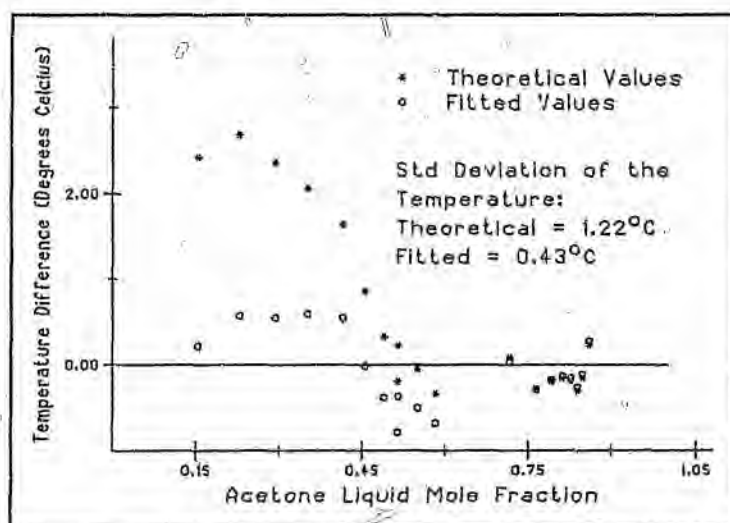
Figure 5.5 The Residual Temperature Plot for the Acetone Benzene System
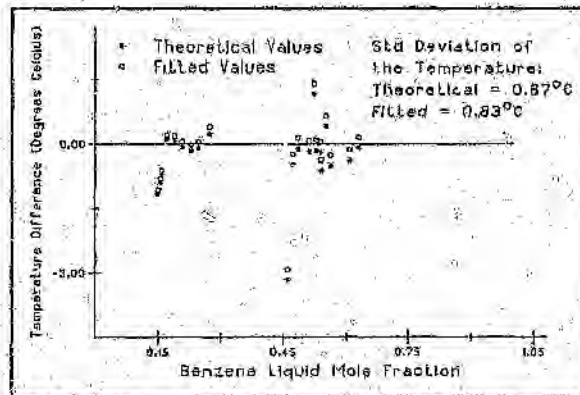
Figure 5.6 The Residual Temperature Plot for the Benzene
Chloroform System
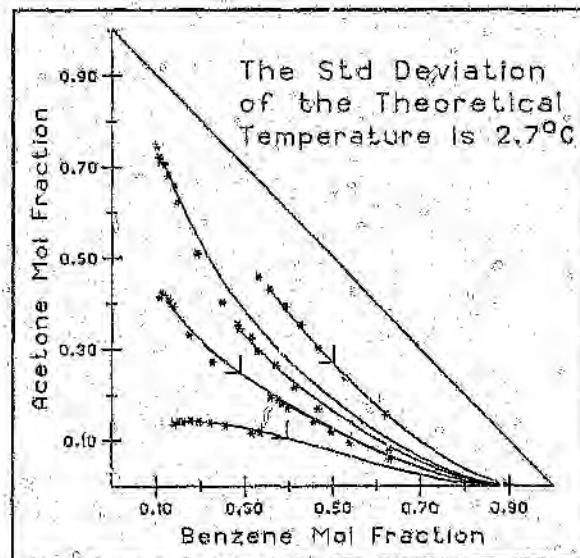
Figure 5.7 The RCM for the Acetone, Benzene and Chloroform
System Simulated with Literature Parameters Compared to
Experimentally Determined Residue Curves (83.6kPa)

The Std Deviation of the Fitted Temperature is $2.35^{\circ}C$
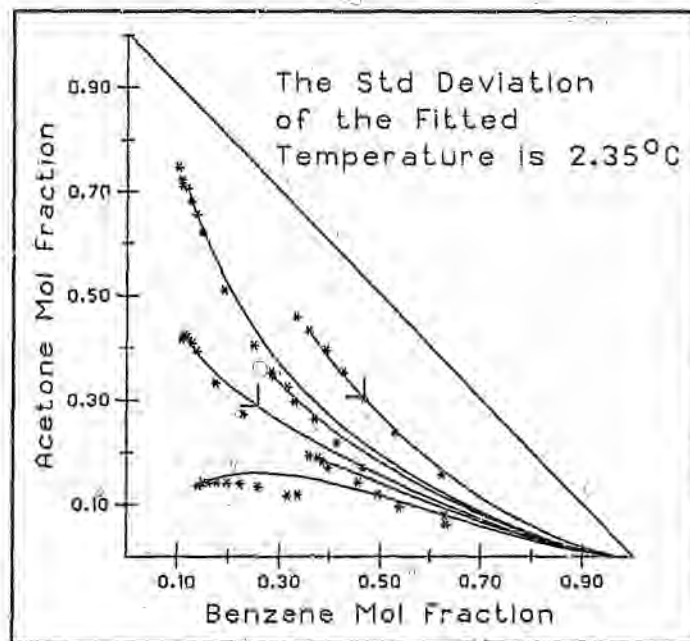
Figure 5.8 The RCM for the Acetone, Benzene and Chloroform System Simulated with Fitted Parameters Compared to Experimentally Determined Residue Curves (83.6kPa)

The ternary system is shown in figures 5.7 and 5.8. Each residue curve is simulated by integrating equation 2.1 using the Margules parameters from literature and those fitted for the binary systems.

In both cases the fits are good indicating that the ternary system was measured accurately. The standard deviations are determined by calculating the predicted temperature at each liquid composition and then applying relevant formulae. Once again some superheating is occurring but it does not seem to change the residue curve map much, indicating that the apparatus is suitable for

measuring residue curve maps as well as giving reasonably accurate VLE data for binary systems.

5.3 The Acetone, Methanol and Chloroform System

The residue curve map for the acetone, methanol and chloroform system is shown in figures 5.9 and 5.10. The values for the fitted model are shown in table 5.3 together with the values from literature (Hirata *et al*, 1975).

Wilson Parameters	Fitted Values	Lit. Values
Λ_{12}	1.3775	0.59963
Λ_{13}	0.6429	1.21619
Λ_{21}	0.2747	0.91281
Λ_{23}	-0.0927	0.10193
Λ_{31}	4.2174	1.49891
Λ_{32}	1.2603	0.88304

where: acetone : 1

methanol : 2

chloroform : 3

Table 5.3 The Fitted and Literature Wilson Parameters for the Acetone, Chloroform and Methanol System

The Std Deviation of the Theoretical Temperature is 2.10°C
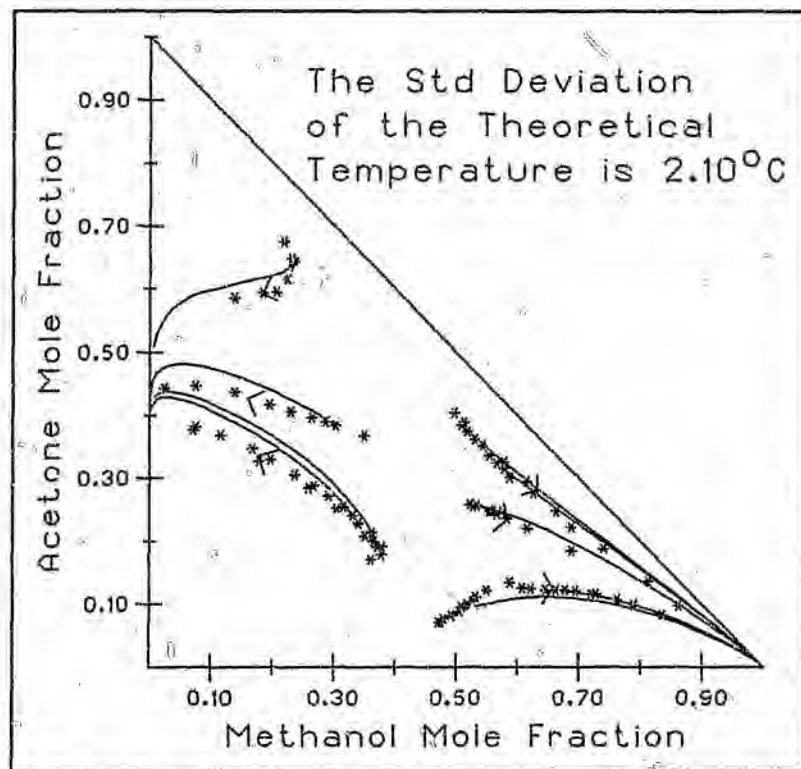
Figure 5.9 The RCM for the Acetone, Methanol and Chloroform System Simulated with Literature Parameters Compared to Experimentally Determined Residue Curves (83.6kPa)
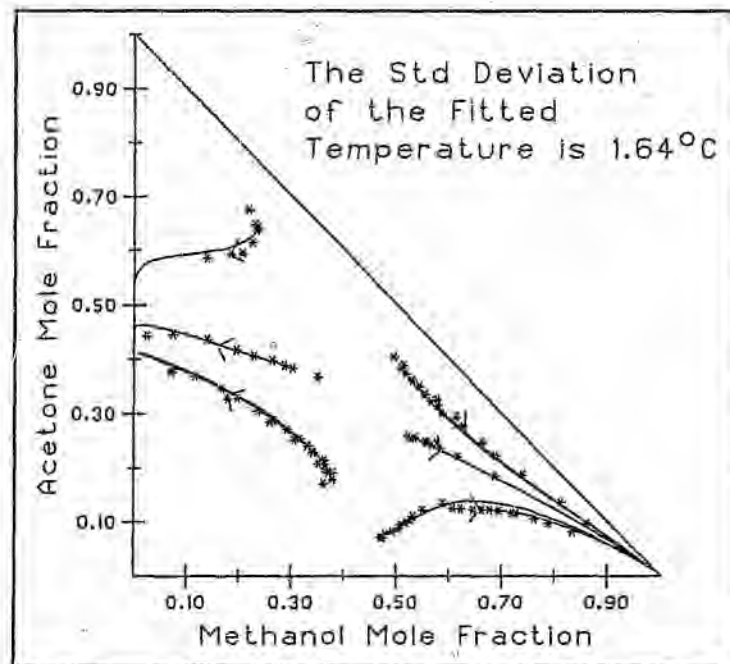
Figure 5.10 The RCM for the Acetone, Chloroform and Methanol System Simulated with Fitted Parameters Compared to Experimentally Determined Residue curves (83.6kPa)

Generally, the residue curve map is well described by both the fitted parameters and the literature parameters. The fitted parameters gives residue curves that are a bit more curved than those of the literature parameters. Both fits are good for the 'straight' residue curves but worse for the areas where the curvature is high. This suggests that the system is not quite at equilibrium in these areas. In order to get more accurate results the boiling rate should be decreased even further when regions of high curvature are encountered.

In general, the apparatus measures a residue curve map that corresponds well to that predicted in the literature and thus the apparatus fulfils the initial aims of this project.

5.4 The 1-Hexene and Methyl Ethyl Ketone System

The measured vapour liquid values as well as the fitted equation are shown in figure 5.11. An azeotrope occurs at a mole fraction of approximately 0.8. The residual temperature plot is shown in figure 5.12. The temperatures are all at most 2 °C greater than those predicted which is within the error expected and thus acceptable.
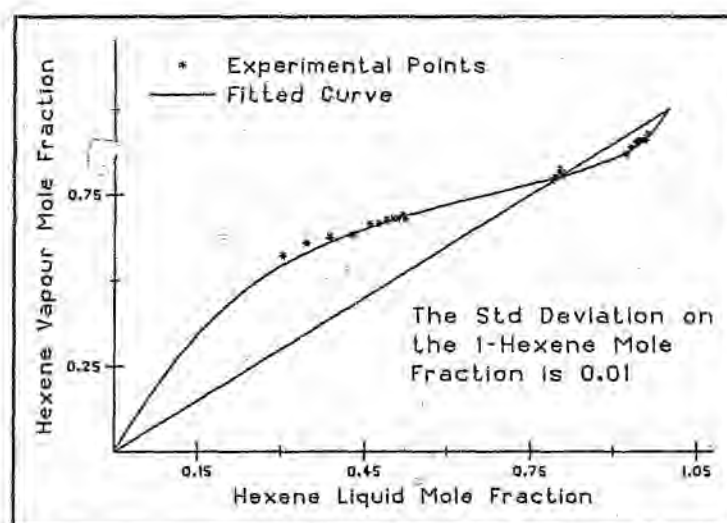
Figure 5.11 The Vapour Liquid Plot for the 1-Hexene Methyl Ethyl Ketone System (83.6kPa)
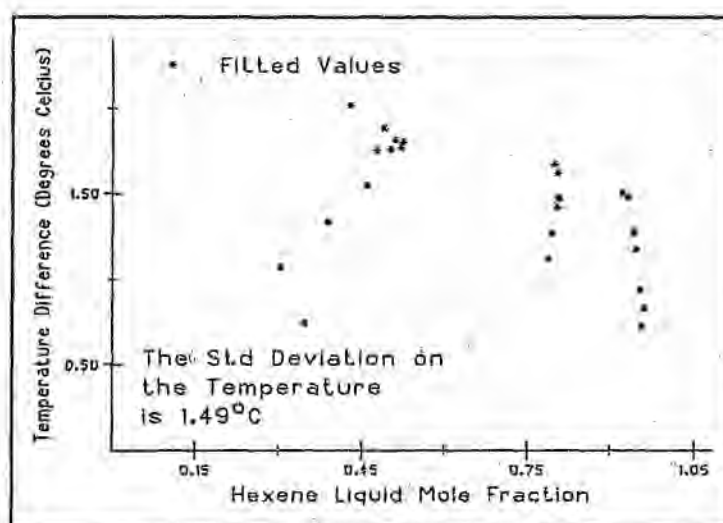
Figure 5.12 The Residual Temperature Plot for the 1-Hexene Methyl Ethyl Ketone System (83.6kPa)

Two entrainers were then considered. The first was acetone, a low boiling entrainer. It is known that acetone does not form an azeotrope with methyl ethyl ketone but its behaviour with 1-hexene is not known (Laroche *et al*, 1992a). This system was thus measured. It should be noted that the system could have been predicted using UNIFAC.

The second entrainer to be considered was butanol, a high boiling entrainer. Correlations in Horsley (1973) suggest that butanol will not form azeotropes with any of the two primary components of the system and thus it would be desirable by the rules of Doherty and Caldarola (1985). This system was thus also measured.

5.4.1 The Acetone, 1-Hexene and Methyl Ethyl Ketone System

The vapour liquid diagrams for the acetone-1-hexene and acetone-methyl ethyl ketone binary systems are shown in figures 5.13 and 5.14. The data for the acetone-methyl ethyl ketone system is not very good as can be seen in figure 5.13. This is probably due to the fact that the heating rate may have been too high and thus the system was not at equilibrium, giving the bad data. A good fit was not obtained and thus published data for this system was used to generate the theoretical curve. These parameters is shown in table 5.4. Despite the bad data, the separation that would be obtained for this system is good as the difference at various points of the vapour and liquid compositions is large. This is illustrated by the high relative volatility of 2.3 at a liquid composition of 0.5.
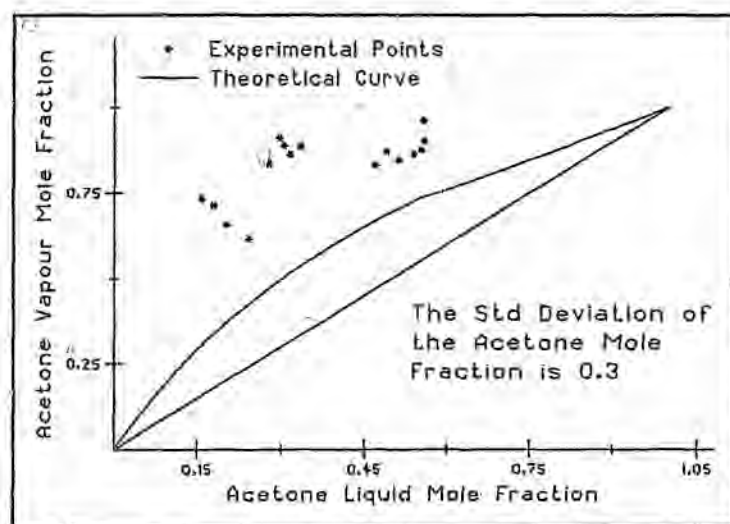
Figure 5.13 The Vapour Liquid Plot for the Acetone Methyl Ethyl Ketone System (83.6kPa)
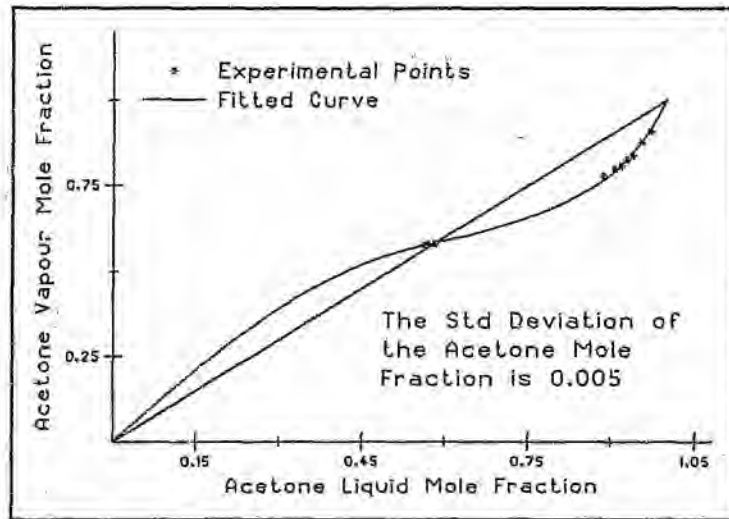
Figure 5.14 The Vapour Liquid Plot for the Acetone 1-Hexene System (83.6kPa)

Λ_{12}	0.3899
Λ_{13}	0.50562
Λ_{21}	0.4157
Λ_{23}	1.0344
Λ_{31}	1.50276
Λ_{32}	0.1806

where : acetone : 1

1-hexene : 2

methyl ethyl ketone : 3

Table 5.4 The Fitted Wilson Parameters for the Acetone, 1-Hexene

and Methyl Ethyl Ketone System

In the case of the acetone-1-hexene system, an azeotrope occurs as may be seen in figure 5.14. This suggests that a separatrix may be introduced into the residue curve map. This is checked for later when the rcm is measured. The model fits well and the parameters are shown in table 5.4.

The residuals for the two systems are shown in figures 5.15 and 5.16. The temperature differences are small, indicating that there is a good agreement with the model.
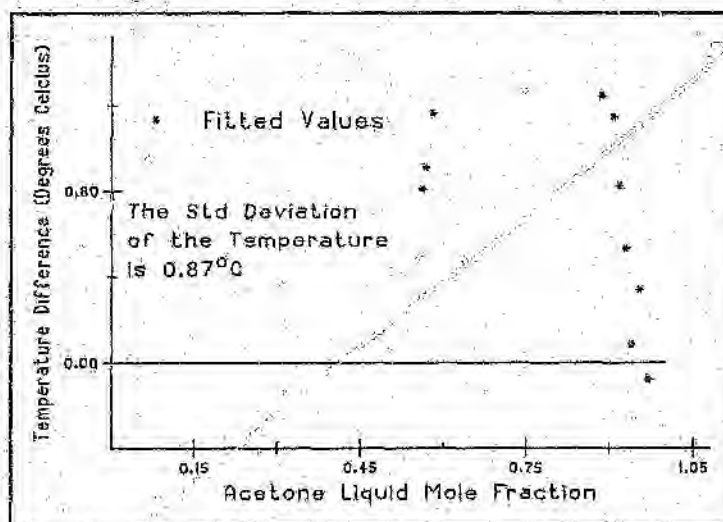
Figure 5.15. The Residual Temperature Plot for the Acetone 1-Hexene System
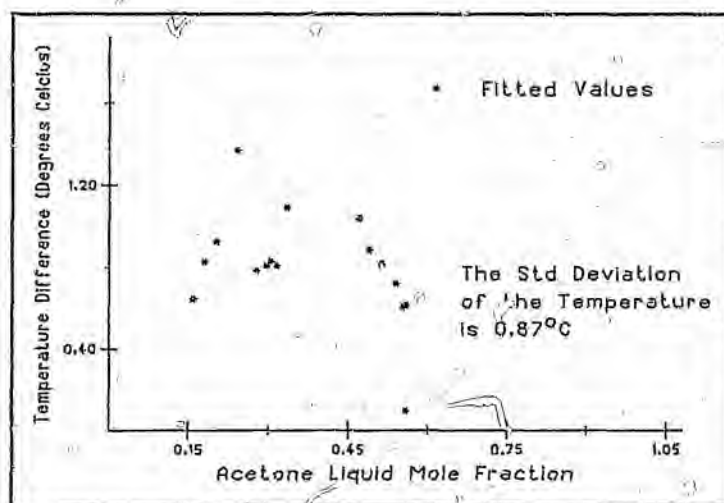
Figure 5.16 The Residual Temperature Plot for the Acetone
Methyl Ethyl Ketone System

The measured residue curve map together with the predicted
residue curves are shown in figure 5.17. The model correlates well
except at regions of high curvature where the system is probably not
in equilibrium.

The Std Deviation
of the Temperature
is 1.19°C
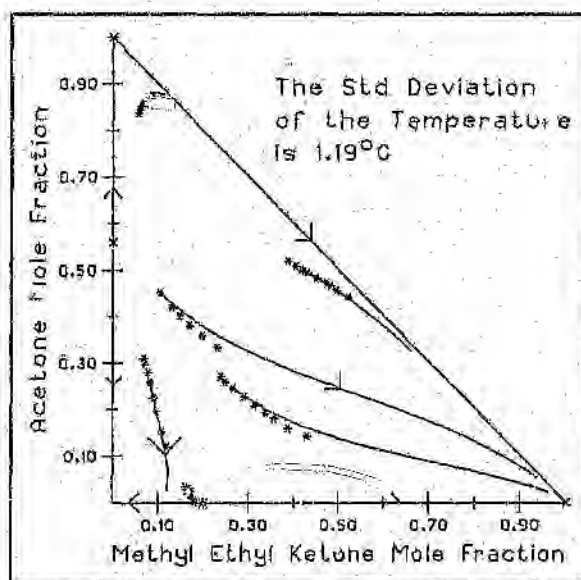
Figure 5.17 The RCM for the Acetone, 1-Hexene and Methyl
Ethyl Ketone System Simulated with Fitted Parameters
Compared to Experimentally Determined Residue Curves
(83.6kPa)

It can be seen that the acetone-1-hexene azeotrope introduces
a separatrix that will prevent separation of methyl ethyl ketone and
1-hexene. As a result, acetone is not a suitable entrainer.

5.4.2 The Butanol, 1-Hexene and Methyl Ethyl Ketone System

The vapour liquid diagrams for the butanol-1-hexene and
butanol-methyl ethyl ketone systems are shown in figures 5.18 and
5.19. In both cases, there was a marked difference in the liquid and
vapour compositions, indicating that good separations will occur. The
relative volatilities for the Butanol 1-Hexene and Butanol Methyl Ethyl

Ketone systems at 0.5 mol 1-Hexene and Methyl Ethyl Ketone respectively are 9 and 7 indicating a good separation. In addition, no azeotropes occur indicating that butanol is a possible entrainer.
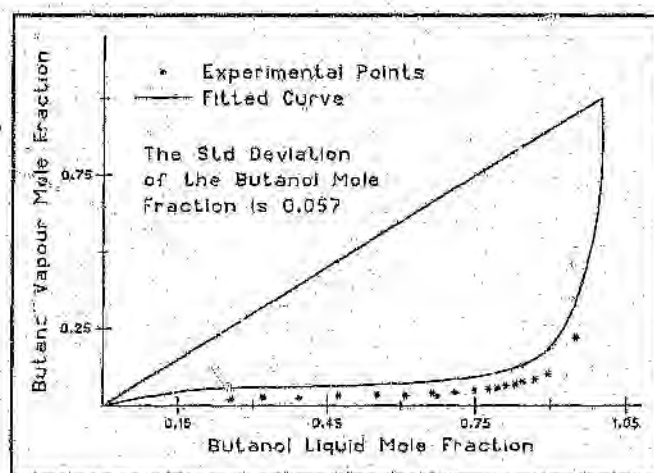
Figure 5.18 The Vapour Liquid Plot for the Butanol 1-Hexene System (83.6kPa)
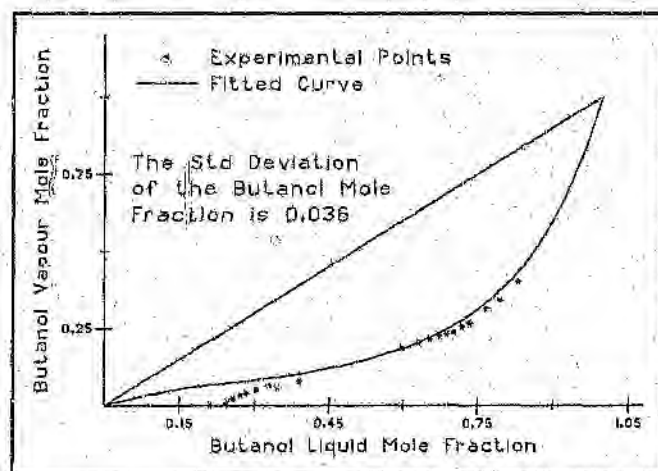
Figure 5.19 The Vapour Liquid Plot for the Butanol Methyl Ethyl Ketone System (83.6kPa)

The fitted curves correlate well with the measured data. The parameters determined are shown in table 5.5. The temperature residuals are shown in figures 5.20 and 5.21. The temperature differences are high indicating that the system was probably superheated. Despite this, the vapour liquid diagrams correlate well with the fitted values.

Λ_{12}	0.0381
Λ_{13}	0.0177
Λ_{21}	0.3886
Λ_{23}	1.0344
Λ_{31}	1.4589
Λ_{32}	0.1806

where : butanol : 1

1-hexene : 2

methyl ethyl ketone : 3

Table 5.5 The Fitted Wilson Parameters for the Butanol, 1-Hexene and Methyl Ethyl Ketone System
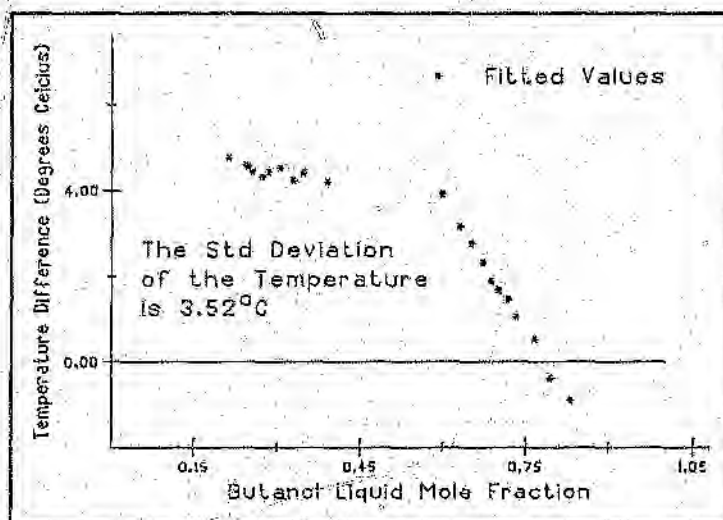
Figure 5.20 The Residual Temperature Plot for the Butanol
Methyl Ethyl Ketone System
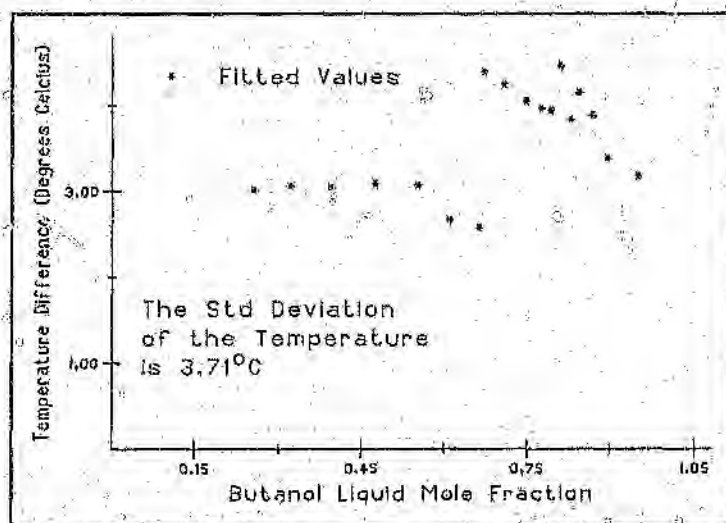
Figure 5.21 The Residual Temperature Plot for the Butanol 1-
Hexene System

The Residue Curve Map was also measured. It is shown in figure 5.22. The predicted residue curves all fit well.
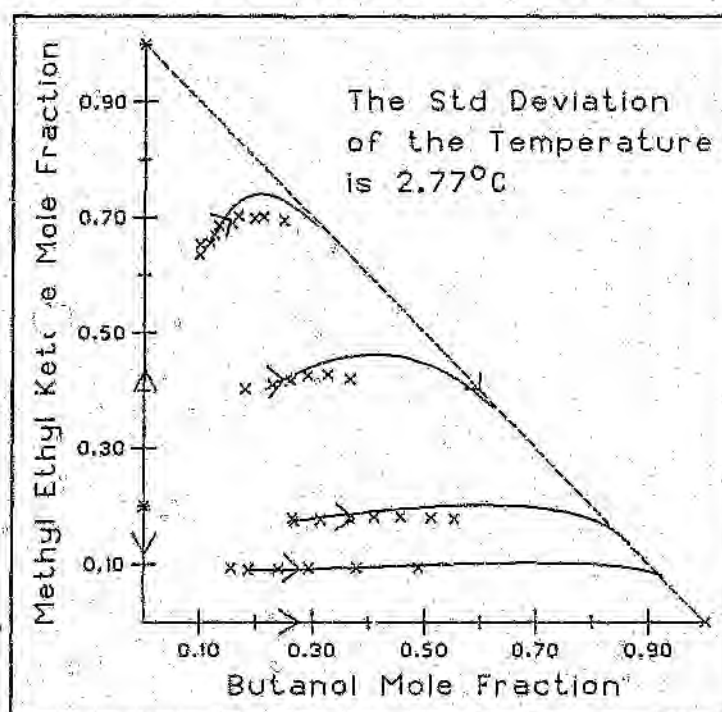
Figure 5.22 The RCM for the Butanol, 1-Hexene and Methyl Ethyl Ketone System Simulated with Fitted Parameters Compared to Experimentally Determined Residue Curves (83.6kPa)

5.5 Concluding Remarks

Initially the apparatus was tested by measuring two known systems. In both cases, the measured results correlated well with published data indicating that the apparatus gives reliable results.

Two different entrainers were then tested for the separation of the 1-hexene and methyl ethyl ketone system. The rcm's generated from the fitted Wilson coefficients are shown in figures 5.23 and 5.24. Acetone introduces a separatrix and is thus not a feasible entrainer. Butanol introduces no additional azeotropes and thus does not introduce a separatrix. It is a promising entrainer that would have to be economically compared to other possible entrainers. A possible column sequence to perform the separation is shown in figure 5.25. The feed to the system is the binary azeotrope with various recycles being used to get the required pure products.
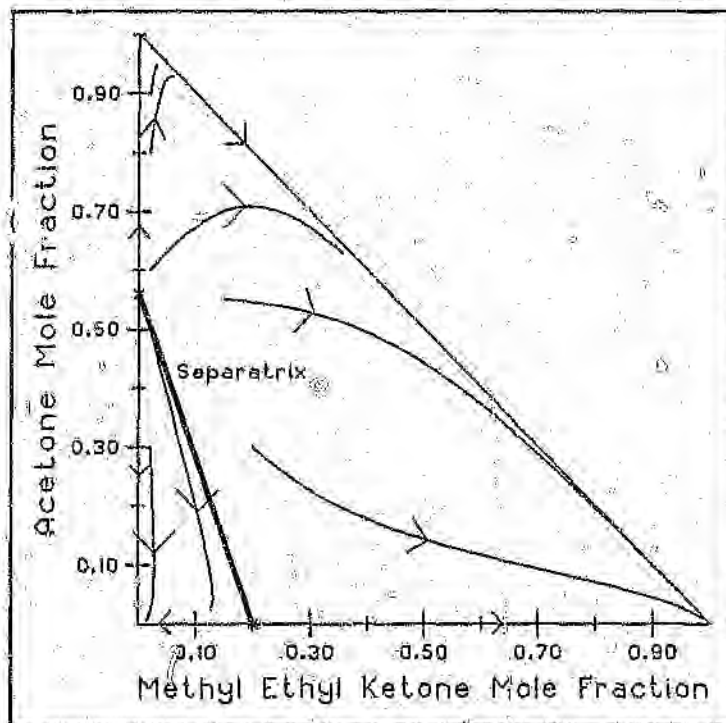
Figure 5.23 The Calculated RCM for the Acetone, 1-Hexene and Methyl Ethyl Ketone System (83.6kPa)
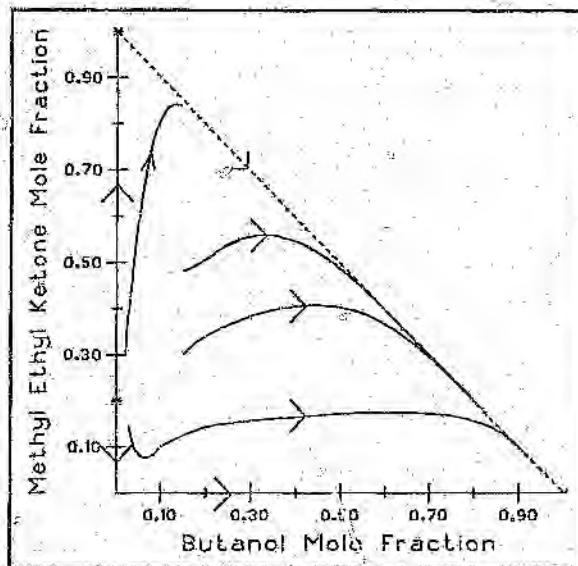
Figure 5.24 The Calculated RCM for the Butanol, 1-Hexene and Methyl Ethyl Ketone System (83.6kPa)
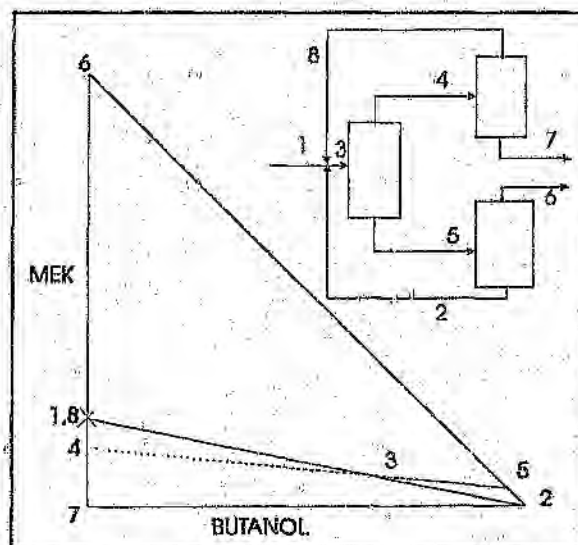
Figure 5.25. The Proposed Separation Sequence for the 1-Hexene, Methyl Ethyl Ketone and Butanol System

Chapter 6
Conclusions and
Recommendations

An apparatus was designed for the measurement of residue curves and the associated VLE data. This apparatus is quick (9 days for a full system), easy and cheap to use and gives reasonably accurate results.

Initially, two systems were measured, the acetone, benzene and chloroform and the acetone, methanol and chloroform systems. The measured results correlate very well with those predicted from the literature, indicating that the results obtained using the designed apparatus are sufficiently accurate.

An entrainer to break the 1-hexene and methyl ethyl ketone azeotrope was then sought and one was found. Butanol is this candidate entrainer with acetone having being tested and discarded as an unsuitable entrainer.

In general, the apparatus performs relatively well, giving good data. There are however a few areas in which improvements may be made.

The required boiling rate can be determined by boiling a pure component and comparing the measured boiling point to published

values. In this way, the heating rate for the initial heating of the charge can be adjusted to give a reasonable boiling temperature and thus reasonable results.

The method of liquid sampling is manual and necessitates the removal of sample of approximately 2ml. Removing such a large sample may disturb the equilibrium in the still, prejudicing the results. It is thus recommended that some method of liquid sampling is introduced that will firstly remov, small amounts of sample and secondly is automated. A possible method of sampling is using a sealed port that takes a small sample and vaporises it, sending the vapour to the GC. This type of sampling should be possible to automate, resulting in runs being done automatically and thus probably more accurately.

Satisfactory results might also be obtained if only liquid compositions were measured. However, due to the differential nature of residue curves if the initial point on a residue curve were inaccurate, the fit to the differential equation might not be good thus giving rise to inaccurate model parameters. In spite of this it would halve the amount of samples that needed to be analysed and in general one would expect the liquid samples to be more accurate than the vapour ones.

It can be seen from the residue curves in the residue curve maps, where only the liquid results are given that the data fits the model results quite well. Whether such good results could have been obtained by regressing only on liquid results is not clear. In fact one

might need to measure more residue curves to obtain equivalent accuracy thus in effect negating the apparent saving in effort of sample analysis.

In conclusion, an apparatus has been designed that can measure residue curves and the associated VLE data easily and quickly. Reasonable results were obtained indicating that the apparatus is useful in the initial search for possible entrainers. There are though some modifications that may be made in further work.

References

Barbosa, D. and M. F. Doherty, 1988, "The Simple Distillation of Homogenous Reactive Mixtures", *Chem. Eng. Sci.*, **43**, pp 541-550

Bekiaris, N., G. A. Meski, C. M. Radu and M. Morari, 1993, "Multiple Steady States in Homogenous Azeotropic Distillation", *Ind. Eng. Chem. Res.*, **32**, pp 2023-2038

Bossen, B. S., S. B. Jorgensen and R. Gani, 1993, "Simulations, Design, and Analysis of Azeotropic Distillation Operations", *Ind. Eng. Chem. Res.*, **32**, pp 620-633

Coulson, J. M. and J. F. Richardson, 1989, *Chemical Engineering Volume 6*, Pergamon Press, Oxford

Doherty, M. F. and J. D. Perkins, 1978a, "On the Dynamics of Distillation Processes - I. The Simple Distillation of Multicomponent Non-Reacting, Homogenous Liquid Mixtures", *Chem. Engng. Sci.*, **33**, pp 281-301

Doherty, M. F. and J. D. Perkins, 1978b, "On the Dynamics of Distillation Processes-II. The Simple Distillation of Model Solutions", *Chem. Engng. Sci.*, **33**, pp 569-578

Doherty, M. F. and J. D. Perkins, 1979, "On the Dynamics of Distillation Processes-III. The Topological Structure of Ternary Residue Curve Maps", *Chem. Engng. Sci.*, **34**, pp 1401-1414

Doherty, M. F. and G. A. Caldarola, 1985, " Design and Synthesis of Homogenous Azeotropic Distillations. 3. The Sequencing of Columns for Azeotropic and Extractive Distillations", *Ind. Eng. Chem. Fundam.*, **24**, pp 474-485

Fien, G. A. F. and Y. A. Liu, 1994, "Heuristic Synthesis and Shortcut Design of Separationb Processes Using Residue Curve Maps: A Review", *Ind. Eng. Chem. Res.*, **33**, pp 2505-2522

Foucher, E. R., M. F. Doherty and M. F. Malone, 1991, "Automatic Screening of Entrainers for Homogenous Azeotropic Distillation", *Ind. Eng. Chem. Res.*, **30**, pp 760-772

Freitag, N. P. and D. B. Robinson, 1986, "Equilibrium Phase Properties of Hydrogen-Methane-Carbon Dioxide, Hydrogen-Carbon Dioxide-n-Pentane and Hydrogen-n-Pentane Systems", *Fluid Phase Equilibria*, **31**, pp 183-201

Guillevic, J. L., D. Richon and H. Renon, 1983, "Vapour-Liquid Equilibrium Measurements upto 558 K and 7 MPa : A New Apparatus", *Ind. Eng. Chem. Fundam.*, **22**, pp 495-499

Hirata, M., S. Ohe and K. Nagahama, 1975, *Computer Aided Data Book of VLE*, Elsevier Scientific Company, Amsterdam

Horsley, A. H., 1973, *Azeotropic Data III, Advances in Chemistry Series 116*, Washington D.C., American Chemical Society, pp 617-627

Inomata, H., K. Tuchiya, K. Arai and S. Saito, 1986, "Measurement of Vapour-Liquid Equilibria at   Temperatures and Pressures using a Flow-Type Apparatus",   *Engineering of Japan*, **19**, pp 386-391

Kalra, H., H. Kubota, D. B. Robinson and   J. Ng, 1978, "Equilibrium Phase Properties of the Carbon Dioxide-n-Heptane System", *J. Chem. Eng. Data*, **23**, pp 317-321

Knapp, J. P. and M. F. Doherty, 1990, "Thermal Integration of Homogenous Azeotropic Distillation Sequences", *AIChE J.*, **36**, pp 969-984

Knight, J. R. and M. F. Doherty, 1989, "Optimal Design and Synthesis of Homogenous Azeotropic Distillation Sequences", *Ind. Eng. Chem. Res.*, **28**, pp 564-572

Laroche, L., N. Bekiaris, H. W. Andersen and M. Morari, 1991, "Homogenous Azeotropic Distillation: Comparing Entrainers", *Can. J. Chem. Eng.*, **69**, pp 1302-1319

Laroche, L., N. Bekiaris, H.W. Andersen and M. Morari, 1992a, "The Curious Behaviour of Homogenous Azeotropic Distillation - Implications for Entrainer Selection", *AIChE J*, **38**, pp 1309 - 1328

Laroche, L., N. Bekiaris, H. W. Andersen and M. Morari, 1992b, "Homogenous Azeotropic Distillation: Separability and Flowsheet Synthesis", *Ind. Eng. Chem. Res.*, **31**, pp 2190-2209

Levy, S. G., D. B. Van Dongen and M. F. Doherty, 1985, "Design and Synthesis of Homogenous Azeotropic Distillations. 2. Minimum Reflux Calculations for Nonideal and Azeotropic Columns", *Ind. Eng. Chem. Fundam.*, **24**, pp 463-474

Muhlbauer, A. L., 1990, "Measurement and Thermodynamic Interpretation of High Pressure Vapour-Liquid Equilibrium", *Thesis*, University of Natal

Nakayama, T., H. Sagara, K. Arai and S. Saito, 1987, "High Pressure Liquid-Liquid Equilibria for the System Water, Ethanol and 1,1-Difureoethane at 323.3 K", *Fluid Phase Equilibria*, **38**, pp 109-127

Ng, H. J. and D. S. Robinson, 1979, "The Equilibrium Phase Properties of Selected Naphthenic Binary Systems : Carbon Dioxide-Methylcyclohexane, Hydrogen Sulphide-Methylcyclohexane", *Fluid Phase Equilibria*, **2**, pp 283-292

Partin, L. E., 1993, "Use Graphical Techniques to Improve Process Analysis", *Chem. Eng. Prog.*, **89**, pp 43-48

Pham, H. H. and M. F. Doherty, 1990a, "Design and Synthesis of Heterogenous Azeotropic Distillations - I. Heterogenous Phase Diagrams", *Chem. Eng. Sci.*, **45**, pp 1823-1836

Pham, H. H. and M. F. Doherty, 1990b, "Design and Synthesis of Heterogenous Azeotropic Distillations - II. Residue Curve Maps", *Chem. Eng. Sci.*, **45**, pp 1837-1843

Pham, H. H. and M. F. Doherty, 1990c, "Design and Synthesis of Heterogenous Azeotropic Distillations - III. Column Sequences", *Chem. Eng. Sci.*, **45**, pp 1845-1854

Ralston, A. and P. Rabinowitz, 1978, *A First Course in Numerical Analysis*, Tokyo, Mcgraw-Hill Kogakusha Ltd., 1978

Reid, R. C, J. M. Prausnitz and B. E. Poling, 1987, *The Properties of Gases and Liquids*, New York, McGraw Hill Inc., pp 254-257, 274-275

Rev, E., 1992, "Crossing of Valleys, Ridges, and Simple Boundaries by Distillation in Homogenous Ternary Mixtures", *Ind. Eng. Chem. Res*, **31**, pp 893-901

Sandler, S. I., 1989, *Chemical Engineering Thermodynamics*, John Wiley and Sons, New York

Stichlmair, J., J. R. Fair and J. L. Bravo, 1989, "Separation of Azeotropic Mixtures via Enhanced Distillation", *Chem. Eng. Prog.*, **85**, pp 63-69

Stichlmair, J. G. and J Herguijuela, 1992, "Separation Regions and Processes of Zeotropic and Azeotropic Ternary Distillation", *AIChE J.*, **38**, pp 1523-1535

Van Dongen, D. B. and M. F. Doherty, 1985a, "On the Dynamics of Distillation Processes - VI. Batch Distillations", *Chem. Eng. Sci.*, **40**, pp 2087-2093

Van Dongen, D. B. and M. F. Doherty, 1983, "Material Stability of Multicomponent Mixtures and the Multiplicity of Solutions to Phase-Equilibrium Equatioons. 1. Nonreacting Mixtures", *Ind. Eng. Chem. Fundam.*, **22**, pp 472-485

Van Dongen, D. B. and M. F. Doherty, 1984, " On The Dynamics of Distillation Processes-V. The topology of the boiling Temperature Surface and its Relation to Azeotropic Distillation", *Chem. Engng. Sci.*, **39**, pp 883-892

Van Dongen, D. B. and M. F. Doherty, 1985b, "Design and Synthesis of Homogenous Azeotropic Distillations. 1. Problem Formulation for A Single Column", *Ind. Eng. Chem. Fundam.*, **24**, pp 454-463

Venimadhavan, G., G. Buzad, M. F. Doherty and M. F. Malone, 1994, "Effect of Kinetics on Residue Curve Maps for Reactive Distillation", *AIChE J.*, **40**, pp 1814-1824

Wahnschafft, O. M., J. W. Koehler, E. Blass and A. W. Westerberg, 1992, "The Product Composition Regions of Single-Feed Azeotropic Distillation Columns", *Ind. Eng. Chem. Res.*, **31**, pp 2345-2362

Young, C. L., 1978, "Experimental Methods for Studying Phase Behaviour of Mixtures at High Temperatures and Pressures", *A Specialist Periodical Report, Vol 2*, pp 71-104

Appendix A

Derivation of the Residue Curve Equation

Consider the simple distillation system shown in figure 2.3. A mass balance on component i will yield:

$$\frac{d(Hx_i)}{dt} = - Vy_i \quad i = 1 \ldots c \qquad \text{A.1}$$

where V is the molar flowrate of the vapour being removed and H is the molar liquid holdup in the still. Equation A.1 may be expanded using the chain rule to give ;

$$\frac{dH}{dt} x_i + H \frac{dx_i}{dt} = -Vy_i \quad i = 1 \ldots c \qquad \text{A.2}$$

An overall mass balance gives :

$$\frac{dH}{dt} = -V \qquad \text{A.3}$$

Combining equation A.2 and A.3 gives :

$$-Vx_i + H\frac{dx_i}{dt} = -Vy_i \qquad\qquad A.4$$

Which reduces to give:

$$\frac{dx_i}{dt} = -\frac{V}{H}(y_i - x_i) \qquad i = 1 \ldots c \qquad\qquad A.5$$

In an isobaric system y_i may be expressed functionally as follows :

$$y_i = y_i(P, T(x), x) \qquad\qquad A.6$$

Equation A.6 is abbreviated and substituted into A.5 to give:

$$\frac{dx_i(t)}{dt} = -\frac{V(t)}{H(t)}(y_i(x(t)) - x_i(t)) \qquad\qquad A.7$$

The liquid holdup and the vapour flow rate may then be incorporated into the derivative and the equation may be generalised

$$\frac{d\overline{x}}{d\xi} = \overline{x} - \overline{y} \qquad\qquad A.8$$

Note that the functional dependences have been left out of equation A.8 for the sake of brevity. Equation A.8 the residue curve equation as described in chapter 2.

Appendix B

Thermodynamic Parameters Used

The parameters used in the Wilson, Margules and Antoine correlations are all presented in this Appendix.

B.1 The Margules Parameters

Acetone = 1

Benzene = 2

Chloroform = 3

Component	Margules Parameter
A_{12}	0.41022
A_{21}	0.38501
A_{13}	-0.69344
A_{31}	-0.58056
A_{23}	-0.21715
A_{32}	-0.20229

Table B.1 The Margules Parameters for the Acetone, Benzene and Chloroform System (Sandler, 1989)

B.2 The Wilson Parameters

Acetone = 1

Methanol = 2

Chloroform = 3

Component	Wilson Parameter
Λ_{12}	0.59963
Λ_{21}	0.91281
Λ_{13}	1.21619
Λ_{31}	1.49891
Λ_{23}	0.10193
Λ_{32}	0.88304

Table B.2. The Wilson Parameters for the Acetone, Methanol and Chloroform System (Hirata *et al*, 1975)

B.3 Antoine Parameters

Table B.3. The Antoine Parameters (Coulson and Richardson, 1989)

Component	AntA	AntB	AntC
Acetone	21.5441	2940.46	-35.93
Benzene	20.7963	2788.15	-52.36
Chloroform	20.8660	2477.07	-39.94

where the Antoine equation used is :

$$\ln P_v = AntA - \frac{AntB}{T + AntC} \qquad \text{B.1}$$

where P_v is in Pascals and T is in Kelvin.

Table B.4. The Antoine Parameters (Hirata *et al*, 1975)

Component	AntA	AntB	AntC
Acetone	7.02447	1161	224
Methanol	7.87863	1473.11	230
Benzene	6.90328	1163.03	227.4
1-Hexene	6.86572	1152.971	225.849
Methyl-Ethyl Ketone	6.97421	1209.6	216
Butan-1-ol	7.65521	1462.060	188.7

where the Antoine equation used is:

$$\log_{10} P_v = AntA - \frac{AntB}{T + AntC}$$ B.2

where P_v is in mmHg and T is in °C.

Appendix C
Computer Programs

The computer programs used were either for simulating the residue curves or for fitting thermodynamic parameters to the measured data. The simulating program was written in Turbo Pascal and the fitting program was written in Matlab.

C.1 The Simulation Program

The program listed below is used to simulate residue curves for the acetone, methanol and chloroform system. It can be adapted to simulate the VLE values only. This is done by removing the integration routine.

```
PROGRAM Residue (INPUT,OUTPUT);

USES Crt;

TYPE

tern = ARRAY[1..3] OF REAL;
cona = ARRAY[1..3,1..3] OF REAL;
```

```
CONST
  antacon : ARRAY[1..3,1..3] OF REAL = ((1 , 1.3775  0.6429)
{1=a}
                              (0.2747 , 1 ,-0.0927 ),  {2=m}
                              (4.2174 ,1.2603 , 1 ));  {3=c}
  A : ARRAY[1..3] OF REAL = (7.02447 ,7.87863  ,6.90328 );
  B : ARRAY[1..3] OF REAL = (1161 ,1473.11  ,1163.03 );
  C : ARRAY[1..3] OF REAL = (224 ,230  ,227.4 );
  syspres = 93600;
  Taz =315;
  Ta=323;
  Tb=353;
  Tc=300;
  fileliq = 'G:\SIM\Liq.DAT';
  filevap = 'G:\sim\Vap.dat';
  frac = 0.01;
  Tcount = 1;

VAR
  xf : tern;
  incr,z : INTEGER;
  file_liq,file_vap,filedat,fileres : TEXT;
  x,y,gamm,pis,xx :tern;
  loop : BOOLEAN;
  Tmax,Tmin,Top,Twrite,delt :REAL;
```

{Procedure to Find the Temperature Extremes}

Procedure Max_Min (VAR Tmax,Tmin : REAL);

BEGIN
  Tmin := Ta;
  IF Tb < Tmin THEN
    Tmin := Tb;
  IF Tc < Tmin THEN
    Tmin := Tc;
  IF Taz < Tmin THEN
    Tmin := Taz;
  Tmax := Ta;
  IF Tb > Tmax THEN
    Tmax := Tb;
  IF Tc > Tmax THEN
    Tmax := Tc;
  IF Taz > Tmax THEN
    Tmax := Taz
END;
{Procedure to Determine the Gamma Value}
Procedure Gamma (x:tern;
          VAR _m :tern);

VAR
  sum1,sum2,sum3 : tern;
  i,j,k : INTEGER;

```
BEGIN
  FOR i := 1 TO 3 DO
    BEGIN
      sum1[i] := 0;
      sum2[i] := 0;
      sum3[i] := 0
    END;
  FOR j := 1 TO 3 DO
    BEGIN
      FOR k := 1 TO 3 DO
        BEGIN
          sum3[j] := x[k]*antacon[j,k] + sum3[j]
        END
    END;
  FOR i := 1 TO 3 DO
    BEGIN
      FOR j := 1 TO 3 DO
        BEGIN
          sum1[i] := x[j]*antacon[j,i]/sum3[j] + sum1[i]
        END
    END;
  FOR i := 1 TO 3 DO
    BEGIN
      FOR j := 1 TO 3 DO
        BEGIN
          sum2[i] := x[j]*antacon[i,j] + sum2[i]
        END
    END;
```

```
FOR i := 1 TO 3 DO
   BEGIN
     gam[i] := exp (1-sum1[i]-ln(sum2[i]))
   END
END;
{Procedure to Determine the Vapour Pressure}
Procedure Antoine (T : REAL;
              VAR P : TERN);


VAR
  component : INTEGER;


BEGIN
  FOR component:=1 TO 3 DO
    P[component]
:=101325/760*exp(ln(10)*(A[component]-(B[component]/(T-273.
15+C[component]))))
END;
{Normalising Procedure}
Procedure Norm (vec :tern;
          VAR vec1 :tern);


VAR
  k : INTEGER;
  vec_sum :REAL;


BEGIN
  vec_sum :=0;
```

```
FOR k := 1 TO 3 DO
  BEGIN
    vec_sum := vec_sum + vec[k]
  END;
FOR k := 1 TO 3 DO
  BEGIN
    vec1[k] := vec[k]/vec_sum
  END
END;
{Procedure to Determine the Vapour Composition}
Procedure Vapour_Comp (Pi,gam,x:tern;
                VAR y:tern);


VAR
  z :INTEGER;
  y1 :tern;


BEGIN
  FOR z:= 1 TO 3 DO
    BEGIN
      y1[z] := Pi[z]*x[z]*gam[z]/syspres
    END;
  Norm(y1,y)
END;
```

```
{Procedure to Integrate the Curve}
Procedure Runge_K_Con (y2,x2 :tern;
                VAR k :tern);


VAR
  b,step : INTEGER;

BEGIN
  step : = 10;
  FOR b : = 1 TO 3 DO
    BEGIN
      k[b] : = step*frac*(y2[b]-x2[b])
    END
END;
{Procedure to Integrate the Curve}
Procedure Runge_Kutta (x3,y3:tern;
                VAR nextx :tern);


VAR
  tcount : REAL;
  h,i: INTEGER;
  xx,k1,k2,k3,k4,k :tern;

BEGIN
  Tcount : = 2;
  Runge_K_Con (y3,x3,k1);
  FOR i: = 1 TO 3 DO
    xx[i]: = x3[i] + 0.5*k1[i];
```

```
Runge_K_Con (y3,xx,k2);
For i: = 1 TO 3 DO
  xx[i]: = x3[i] + 0.5*k2[i];
Runge_K_Con (y3,xx,k3);
For i: = 1 TO 3 DO
  xx[i]: = x3[i] + k3[i];
Runge_K_Con (y3,xx,k4);
For i: = 1 TO 3 DO
  k[i]: = (k1[i] + 2*k2[i] + 2*k3[i] + k4[i])/6;
For i: = 1 TO 3 DO
  nextx[i]: = x3[i] + k[i];
Norm (nextx,nextx);
IF (x[1] < 0.0001) OR (x[2] < 0.0001) OR (x[3] < 0.0001)
THEN
  BEGIN
    loop : = false
  END


END;
{Procedure to Determine the Temperature at the Point}
Procedure Temperature (Tmin,Tmax :REAL;
                  x,gamma:tern;
                  VAR Temp:REAL);


VAR
nextT,nextY,Y_int,slope,leftT,rightT,leftY,rightY : REAL;
```

```
FUNCTION Pres(x,gamma:tern;
         T1:REAL):REAL;


VAR
  i:INTEGER;
  P :REAL;
  ParP :tern;


BEGIN
  P: .0;
  Antoine(T1,ParP);
  FOR i: = 1 TO 3 DO
    BEGIN
      P: =P+x[i]*ParP[i]*gamma[i]
    END;
  Pres: =P
END;


BEGIN
  leftT: = Tmin;
  rightT: = Tmax;
  REPEAT
    leftY  : = syspres-Pres(x,gamma,leftT);
    rightY: = syspres-Pres(x,gamma,rightT);
    slope  : = (leftY-rightY)/(leftT-rightT);
    Y_Int : =  leftY-slope*leftT;
    nextT : = -Y_Int/slope;
    nextY : = syspres-Pres(x,gamma,nextT);
```

```
       IF nextT*leftT<0 THEN
         BEGIN
           rightT: =nextT;
           righty: =nextY
         END
       ELSE
         BEGIN
           leftT: =nextT;
           leftY: =nextY
         END
     UNTIL (ABS(nextY)<0.0001);
      Temp : = nextT
   END;
   {The Main Program Body}
   BEGIN
     z := 1;
     Assign (filedat,'g:\sim\amcr.dta');
     Reset (filedat);
     Assign (fileres,'g:\sim\amcrr2.dta');
     Rewrite (fileres);
     WHILE not eof(filedat) DO
       BEGIN
         WRITELN (z);
         WRITELn (fileres,z);
         z := z+1;
         READ (filedat,xf[1]);
         READ (filedat,xf[2]);
         READLN (filedat,xf[3]);
```

```
        loop := true;
        Max_Min (Tmax,Tmin);
        x := xf;
        Gamma(x,gamm);
        Temperature (Tmin,Tmax,x,gamm,Top);
        Twrite := Top - 0.5;
      REPEAT
        Gamma(x,gamm);
        Temperature (Tmin,Tmax,x,gamm,Top);
        Antoine (Top,Pis);
        Vapour_Comp(Pis,Gamm,x,y);
        Runge_Kutta(x,y,xx);
        IF (Top > Twrite) THEN
          BEGIN
            Twrite := Twrite + Tcount;
            Writeln(fileres,x[2]:8:4,' ',x[1]:8:4);

Writeln(x[3]:8:4,x[2]:8:4,x[1]:8:4,y[3]:8:4,y[2]:8:4,y[1]:8:4,(Top-2
73.15):7:3);
          END;
        x := xx;
      UNTIL (loop = false);
      END;
    Close(filedat);
    Close(fileres)
  END.
```

C.2 The Parameter Fitting Programs

The following program was written to determine the parameters for the acetone, methanol and chloroform system.

Main Program
%Definitions & InitialisationsAcetone,Chloroform,Benzene

```
A12 = 0.0051277;
A13 = -0.8871;
A21 = 0.4302284;
A23 = -0.180261;
A31 = -0.84;
A32 = -0.180135;


A0(1) = A12;
A0(2) = A13;
A0(3) = A21;
A0(4) = A23;
A0(5) = A31;
A0(6) = A32;


load temp2.asc


x1   = temp2(:,1);  %Acetone
x2   = temp2(:,2);  %Benzene
x3   = temp2(:,3);  %Chloroform
y1   = temp2(:,4);
```

```
y2 = temp2(:,5);
y3 = temp2(:,6);
T = temp2(:,7);


options(1)  = 0;
options(14) = 1000; % Maximum iterations
options(2) = 1e-10;
options(3) = 1e-2;


[A,options] = fmins('mindiff2',A0,options,[],x1,x2,x3,y1,y2,y3,T);


disp (A)
disp (options);
```

Procedure mindiff2

```
function Error = fun(A0,x1,x2,x3,y1,y2,y3,T);


options(1) = 0;
options(2) = 1e-6;
z = length(T);
disp (z);
gamm1 = exp((1 - x1) .* (2 .* x1 .* ( x2 .* A0(3) + x3 .* A0(5))
    + A0(1) .* x2 .* (1 - 2 .* x1) + A0(2) .* x3 .* (1-2 .* x1)));
gamm2 = exp((1 - x2) .* (2 .* x2 .* (x1 .* A0(1) + x3 .* A0(6))
    + A0(3) .* x1 .* (1 - 2 .* x2) + A0(4) .* x3 .* (1-2 .* x2)));
gamm3 = exp((1 - x3) .* (2 .* x3 .* (x2 .* A0(4) + x1 .* A0(2))
    + A0(6) .* x2 .* (1 - 2 .* x3) + A0(5) .* x1 .* (1-2 .* x3)));
```

```
for i = 1:z,
ttt(i) =
fmins('temp',T(i),options,[],gamm1(i),gamm2(i),gamm3(i),x1(i),x2(i
),x3(i));
end;
vap1 = exp ( 21.5441 - 2940.46 ./ (ttt - 35.93 + 273.15));
vap2 = exp ( 20.7963 - 2788.15 ./ (ttt - 52.36 + 273.15));
vap3 = exp ( 20.8660 - 2696.79 ./ (ttt - 46.16 + 273.15));
yy1 = (gamm1 .* vap1' .* x1) ./ 83600;
yy2 = (gamm2 .* vap2' .* x2) ./ 83600;
yy3 = (gamm3 .* vap3' .* x3) ./ 83600;
Err1 = (y1 - yy1)./0.02;
Err2 = (y2 - yy2)./0.02;
Err3 = (y3 - yy3)./0.02;
Err4 = (T - ttt')./2;
Error = Err1(:)'*Err1(:) + Err2(:)'*Err2(:) + Err3(:)'*Err3(:)
 + Err4(:)'*Err3(:);
```

Procedure temp

```
function temp = fun(T,gamm1,gamm2,gamm3,x1,x2,x3);
vap1 = exp ( 21.5441 - 2940.46 / (T - 35.93 + 273.15));
vap2 = exp ( 20.7963 - 2788.15 / (T - 52.36 + 273.15));
vap3 = exp ( 20.8660 - 2696.79 / (T - 46.16 + 273.15));
temp =abs( x1 * vap1 * gamm1 + x2 * vap2 * gamm2 + x3 *
gamm3 * vap3 - 83600);
```

Appendix D
The Still Design

The dimensioned designs of the large and small stills are shown in figure D.1 and D.2. Note that the internals of the still are all in one piece and can thus be removed for cleaning.
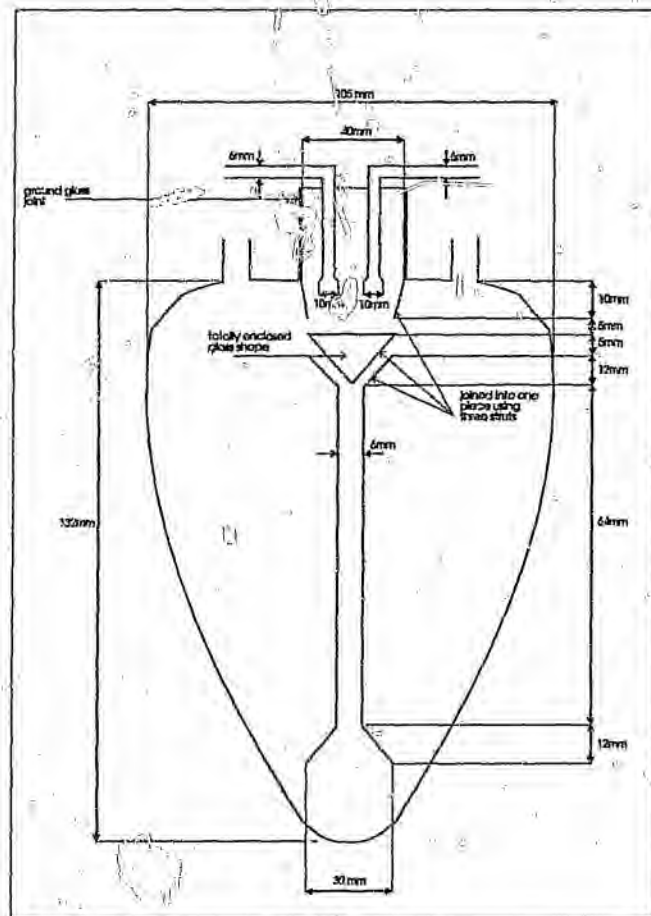
Figure D.1 The Small Still
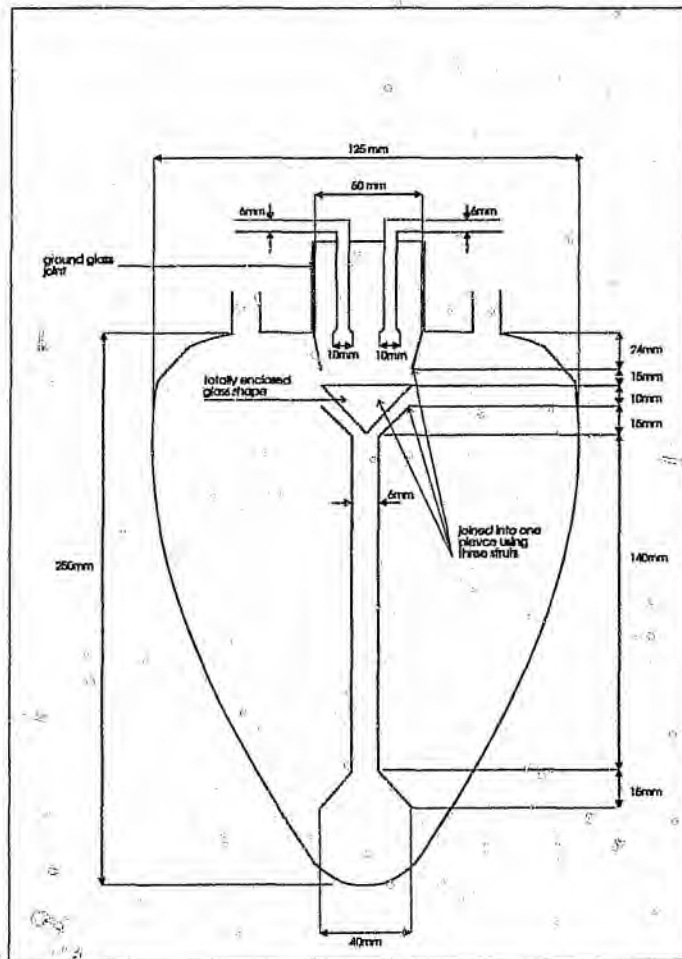
Figure D.2 The Large Still

Appendix E

Experimental Results

	Liquid Frac			Vapour Frac			
	Ace-tone	Ben-zene	Chloro-form	Ace-tone	Ben-zene	Chloro-form	Temp
Run 1	0.746	0.101	0.153	0.791	0.079	0.130	54
	0.722	0.106	0.172	0.793	0.081	0.126	54.5
	0.710	0.109	0.181	0.785	0.085	0.130	55
	0.706	0.118	0.176	0.781	0.089	0.131	58
	0.681	0.125	0.194	0.765	0.094	0.141	59.5
	0.656	0.137	0.207	0.741	0.103	0.156	61.5
	0.621	0.147	0.232	0.707	0.113	0.180	61.5
	0.510	0.191	0.299	0.610	0.141	0.249	62.5
	0.406	0.249	0.348	0.527	0.169	0.304	64.5
Run 2	0.415	0.108	0.477	0.549	0.058	0.393	58
	0.424	0.112	0.464	0.481	0.086	0.433	58
	0.419	0.118	0.463	0.478	0.089	0.433	58.5
	0.409	0.128	0.463	0.459	0.096	0.444	58.75
	0.394	0.138	0.468	0.440	0.103	0.457	59
	0.332	0.174	0.494	0.376	0.129	0.494	65
	0.272	0.227	0.501	0.326	0.160	0.514	67.5

Table E.1 The Experimental Results for the Ternary Acetone, Benzene and Chloroform System

	Liquid Frac			Vapour Frac			
	Ace-tone	Ben-zene	Chloro-form	Ace-tone	Ben-zene	Chloro-form	Temp
Run 3	0.458	0.332	0.210	0.580	0.232	0.188	58
	0.431	0.357	0.212	0.564	0.255	0.181	58.5
	0.395	0.392	0.213	0.536	0.274	0.190	59
	0.353	0.426	0.221	0.493	0.305	0.202	60
	0.303	0.466	0.230	0.438	0.342	0.221	61.5
	0.237	0.529	0.235	0.374	0.387	0.238	62.5
	0.157	0.621	0.223	0.286	0.457	0.257	64.5
Run 4	0.136	0.141	0.722	0.097	0.051	0.852	55
	0.142	0.150	0.707	0.125	0.091	0.784	59
	0.141	0.161	0.698	0.134	0.105	0.761	60
	0.143	0.177	0.680	0.140	0.122	0.739	60
	0.141	0.197	0.662	0.144	0.139	0.718	60.5
	0.139	0.222	0.639	0.145	0.161	0.694	61
	0.133	0.257	0.610	0.144	0.181	0.674	61.5
	0.116	0.316	0.568	0.139	0.219	0.642	62
	0.118	0.336	0.547	0.121	0.285	0.593	66
Run 5	0.193	0.358	0.449	0.300	0.216	0.484	59.5
	0.189	0.376	0.435	0.249	0.270	0.481	61.5
	0.181	0.384	0.435	0.238	0.284	0.478	61.75
	0.171	0.396	0.433	0.228	0.295	0.477	62
	0.142	0.456	0.402	0.196	0.338	0.466	63.5
	0.119	0.496	0.385	0.174	0.369	0.457	64
	0.095	0.538	0.367	0.150	0.407	0.443	65
	0.060	0.630	0.310	0.150	0.407	0.443	66

Table E.2 The Experimental Results for the Acetone, Benzene and Chloroform System

	Liquid Frac			Vapour Frac			
	Ace-tone	Ben-zene	Chloro-form	Ace-tone	Ben-zene	Chloro-form	Temp
Run 6	0.353	0.283	0.365	0.439	0.191	0.371	59.5
	0.345	0.287	0.368	0.448	0.207	0.345	60
	0.325	0.314	0.361	0.428	0.225	0.348	60.5
	0.296	0.329	0.375	0.396	0.241	0.362	60.5
	0.263	0.370	0.367	0.362	0.261	0.377	61
	0.218	0.413	0.369	0.313	0.296	0.391	62
	0.170	0.465	0.365	0.258	0.343	0.399	63
	0.078	0.628	0.294	0.170	0.443	0.387	65

Table E.3 The Experimental Results for the Ternary Acetone, Benzene and Chloroform System

Liquid Frac			Vapour Frac			
Ace- tone	Ben- zene	Chloro- form	Ace- tone	Ben- zene	Chloro- form	Temp
0.860	0.140	0.000	0.905	0.095	0.000	52.45
0.848	0.152	0.000	0.900	0.100	0.000	52.2
0.839	0.161	0.000	0.894	0.106	0.000	52.15
0.827	0.173	0.000	0.890	0.110	0.000	52.4
0.812	0.188	0.000	0.879	0.121	0.000	52.6
0.792	0.208	0.000	0.869	0.131	0.000	52.8
0.764	0.236	0.000	0.854	0.146	0.000	53.05
0.717	0.283	0.000	0.828	0.172	0.000	54
0.583	0.417	0.000	0.775	0.225	0.000	55.45
0.550	0.450	0.000	0.769	0.231	0.000	56.25
0.514	0.486	0.000	0.749	0.251	0.000	56.7
0.515	0.485	0.000	0.757	0.243	0.000	57.1
0.489	0.511	0.000	0.677	0.323	0.000	57.65
0.455	0.545	0.000	0.694	0.306	0.000	58.8
0.415	0.585	0.000	0.713	0.287	0.000	60.35
0.351	0.649	0.000	0.678	0.322	0.000	62.15
0.292	0.708	0.000	0.709	0.291	0.000	63.9
0.228	0.772	0.000	0.636	0.364	0.000	66.05
0.154	0.846	0.000	0.499	0.501	0.000	68.35

Run 1 begins at the first data row (0.860) and Run 2 begins at the row 0.583.

Table E.4 The Experimental Data for the Acetone and Benzene Binary System

	Liquid Frac			Vapour Frac			
	Ace-tone	Ben-zene	Chloro-form	Ace-tone	Ben-zene	Chloro-form	Temp
Run 1	0.900	0.000	0.100	0.898	0.000	0.102	53.8
	0.808	0.000	0.192	0.870	0.000	0.130	54.3
	0.793	0.000	0.207	0.854	0.000	0.146	56.6
	0.766	0.000	0.234	0.832	0.000	0.168	59.15
	0.719	0.000	0.281	0.808	0.000	0.192	59.8
	0.688	0.000	0.312	0.790	0.000	0.210	60.2
	0.604	0.000	0.396	0.682	0.000	0.318	66.5
Run 2	0.442	0.000	0.558	0.482	0.000	0.518	58.45
	0.469	0.000	0.541	0.474	0.000	0.526	60.2
	0.446	0.000	0.554	0.463	0.000	0.537	62.4
	0.431	0.000	0.569	0.449	0.000	0.551	63.2
	0.409	0.000	0.591	0.425	0.000	0.575	65.1
Run 3	0.288	0.000	0.712	0.233	0.000	0.767	58
	0.273	0.000	0.727	0.236	0.000	0.764	58.2
	0.273	0.000	0.727	0.246	0.000	0.754	58.45
	0.283	0.000	0.717	0.258	0.000	0.742	58.65
	0.290	0.000	0.710	0.271	0.000	0.729	60.2
	0.663	0.000	0.337	0.776	0.000	0.224	58.8

Table E.5 The Experimental Results for the Acetone and Chloroform Binary System

	Liquid Frac			Vapour Frac			
	Ace-tone	Ben-zene	Chloro-form	Ace-tone	Ben-zene	Chloro-form	Temp
Run 4	0.831	0.000	0.169	0.926	0.000	0.074	54.1
	0.848	0.000	0.152	0.911	0.000	0.089	53.8
	0.822	0.000	0.178	0.896	0.000	0.104	54.1
	0.800	0.000	0.200	0.879	0.000	0.121	54.55
	0.768	0.000	0.232	0.862	0.000	0.138	55.1
	0.720	0.000	0.280	0.847	0.000	0.153	55.9
	0.663	0.000	0.337	0.776	0.000	0.224	58.8

Table E.6 The Experimental Results for the Acetone and Chloroform System

	Liquid Frac			Vapour Frac			
	Ace-tone	Ben-zene	Chloro-form	Ace-tone	Ben-zene	Chloro-form	Temp
Run 1	0.000	0.150	0.850	0.000	0.062	0.938	57.4
	0.000	0.155	0.845	0.000	0.067	0.933	57.7
	0.000	0.158	0.842	0.000	0.067	0.933	58
	0.000	0.171	0.829	0.000	0.088	0.912	59.05
	0.000	0.189	0.811	0.000	0.099	0.901	59.35
	0.000	0.207	0.793	0.000	0.106	0.894	59.55
	0.000	0.228	0.772	0.000	0.115	0.885	59.85
	0.000	0.246	0.754	0.000	0.128	0.872	60.25
	0.000	0.273	0.727	0.000	0.148	0.852	61.1
Run 2	0.000	0.461	0.539	0.000	0.211	0.789	61.35
	0.000	0.472	0.528	0.000	0.307	0.693	64.25
	0.000	0.484	0.516	0.000	0.316	0.684	64.85
	0.000	0.511	0.489	0.000	0.329	0.671	65.3
	0.000	0.539	0.461	0.000	0.339	0.661	65.4
	0.000	0.528	0.472	0.000	0.348	0.652	65.65
	0.000	0.538	0.462	0.000	0.361	0.639	65.8
	0.000	0.562	0.438	0.000	0.371	0.629	65.95
	0.000	0.551	0.449	0.000	0.388	0.612	66.65
	0.000	0.522	0.478	0.000	0.289	0.711	66.85
	0.000	0.608	0.392	0.000	0.412	0.588	66.95
	0.000	0.630	0.370	0.000	0.455	0.545	67.65

Table E.7 The Experimental Results for the Benzene and Chloroform Binary System

	Liquid Frac			Vapour Frac			
	Ace-tone	Meth-anol	Chloro-form	Ace-tone	Meth-anol	Chloro-form	Temp
Run 1	0.675	0.218	0.107	0.703	0.223	0.074	51.85
	0.648	0.230	0.121	0.694	0.233	0.073	51.95
	0.642	0.236	0.122	0.680	0.246	0.074	51.95
	0.639	0.234	0.127	0.669	0.256	0.075	52
	0.637	0.234	0.129	0.662	0.258	0.080	52
	0.616	0.225	0.160	0.653	0.256	0.090	52.05
	0.595	0.206	0.199	0.587	0.236	0.178	53.15
	0.593	0.184	0.223	0.624	0.232	0.144	56.25
	0.586	0.138	0.276	0.562	0.215	0.224	57.2
Run 2	0.326	0.578	0.097	0.438	0.417	0.145	52.95
	0.314	0.578	0.108	0.398	0.482	0.120	53.1
	0.294	0.614	0.092	0.376	0.506	0.118	53
	0.277	0.627	0.096	0.320	0.479	0.202	52.85
	0.247	0.664	0.089	0.335	0.560	0.105	53
	0.222	0.688	0.090	0.310	0.584	0.106	55.65
	0.188	0.740	0.072	0.279	0.619	0.103	56.65
	0.136	0.813	0.051	0.238	0.675	0.088	57.15
	0.097	0.862	0.041	0.196	0.731	0.073	58.1

Table E.8 The Experimental Results for the Acetone, Methanol and Chloroform System

	Liquid Frac			Vapour Fraction			
	Ace-tone	Meth-anol	Chlor-oform	Ace-tone	Meth-anol	Chlor-oform	Temp
Run 3	0.367	0.350	0.283	0.369	0.332	0.300	53.4
	0.384	0.303	0.313	0.371	0.355	0.275	53.7
	0.389	0.287	0.324	0.373	0.346	0.280	53.7
	0.396	0.264	0.339	0.377	0.337	0.286	53.7
	0.406	0.230	0.365	0.385	0.314	0.301	53.95
	0.417	0.195	0.388	0.394	0.288	0.317	54.3
	0.436	0.138	0.425	0.410	0.259	0.331	54.9
	0.446	0.075	0.479	0.431	0.215	0.355	55.8
	0.443	0.024	0.533	0.460	0.174	0.366	56.95
Run 4	0.125	0.608	0.267	0.111	0.539	0.350	53.3
	0.124	0.622	0.254	0.114	0.550	0.336	53.5
	0.122	0.646	0.232	0.118	0.563	0.319	53.4
	0.122	0.663	0.215	0.123	0.573	0.303	53.6
	0.122	0.678	0.200	0.128	0.586	0.286	53.75
	0.120	0.695	0.185	0.131	0.600	0.269	55.2
	0.116	0.720	0.164	0.133	0.613	0.254	57.8
	0.115	0.728	0.156	0.134	0.631	0.234	58.2
	0.106	0.763	0.131	0.135	0.649	0.216	58.65
	0.098	0.790	0.112	0.134	0.673	0.194	59.25
	0.082	0.835	0.083	0.124	0.715	0.160	61.6

Table E.9 The Experimental Results for the Acetone, Methanol and Chloroform Ternary System

	Liquid Frac			Vapour Frac			
	Ace-tone	Meth-anol	Chloro-form	Ace-tone	Meth-anol	Chloro-form	Temp
Run 5	0.255	0.529	0.216	0.281	0.473	0.246	53.05
	0.258	0.523	0.218	0.271	0.500	0.229	53.2
	0.256	0.534	0.210	0.267	0.512	0.221	53.2
	0.248	0.555	0.196	0.263	0.521	0.216	53
	0.246	0.559	0.195	0.262	0.526	0.212	53.1
	0.242	0.567	0.191	0.259	0.532	0.209	56
	0.236	0.583	0.182	0.255	0.543	0.202	58.15
	0.219	0.616	0.165	0.248	0.558	0.194	59.05
	0.184	0.688	0.127	0.239	0.582	0.178	59.65
Run 6	0.190	0.379	0.431	0.137	0.383	0.480	52.5
	0.208	0.351	0.441	0.151	0.396	0.453	52.5
	0.227	0.341	0.432	0.168	0.396	0.436	52.7
	0.252	0.305	0.443	0.193	0.380	0.427	54.4
	0.284	0.259	0.456	0.225	0.351	0.424	57.5
	0.326	0.178	0.495	0.255	0.315	0.429	58.35
	0.377	0.071	0.552	0.282	0.295	0.423	56.6

Table E.10 The Experimental Results for the Acetone, Methanol and Chloroform Ternary System

	Liquid Frac			Vapour Frac			
	Ace-tone	Meth-anol	Chloro-form	Ace-tone	Meth-anol	Chloro-form	Temp
Run 7	0.170	0.362	0.468	0.095	0.364	0.541	51.7
	0.179	0.378	0.443	0.117	0.389	0.494	52.4
	0.190	0.371	0.438	0.126	0.399	0.474	52.35
	0.199	0.365	0.436	0.132	0.409	0.458	52.5
	0.206	0.363	0.431	0.137	0.415	0.449	52.2
	0.213	0.362	0.425	0.145	0.416	0.438	52.25
	0.229	0.340	0.431	0.153	0.420	0.427	52.3
	0.240	0.331	0.429	0.169	0.412	0.419	52.4
	0.254	0.316	0.430	0.173	0.415	0.412	52.65
	0.271	0.292	0.437	0.178	0.421	0.401	52.7
	0.287	0.267	0.446	0.171	0.433	0.396	52.7
	0.306	0.236	0.459	0.191	0.419	0.390	53.15
	0.329	0.197	0.474	0.200	0.419	0.381	53.65
	0.346	0.167	0.487	0.191	0.431	0.378	54.25
	0.369	0.116	0.516	0.229	0.401	0.370	54.95
	0.382	0.077	0.541	0.216	0.423	0.361	55.85

Table E.11 The Experimental Results for the Acetone, Methanol and Chloroform Ternary System

	Liquid Frac			Vapour Frac			
	Ace-tone	Meth-anol	Chloro-form	Ace-tone	Meth-anol	Chloro-form	Temp
Run 8	0.404	0.496	0.100	0.499	0.417	0.083	52.4
	0.389	0.514	0.098	0.476	0.440	0.085	52.5
	0.384	0.509	0.107	0.462	0.453	0.085	52.55
	0.374	0.518	0.108	0.450	0.465	0.086	52.6
	0.362	0.531	0.108	0.431	0.479	0.090	52.65
	0.351	0.543	0.106	0.420	0.485	0.095	52.7
	0.336	0.554	0.110	0.394	0.503	0.102	52.7
	0.324	0.566	0.110	0.379	0.516	0.104	52.75
	0.300	0.588	0.112	0.357	0.531	0.112	52.6
Run 9	0.071	0.476	0.453	0.030	0.386	0.583	50.5
	0.071	0.472	0.457	0.033	0.404	0.563	50.7
	0.077	0.479	0.444	0.037	0.423	0.540	50.9
	0.082	0.492	0.42	0.042	0.437	0.521	51.05
	0.088	0.505	0.408	0.047	0.448	0.505	51.05
	0.094	0.509	0.397	0.050	0.455	0.495	.1
	0.100	0.518	0.382	0.058	0.464	0.479	51.25
	0.104	0.527	0.369	0.061	0.471	0.469	51
	0.110	0.532	0.358	0.073	0.487	0.440	52
	0.122	0.551	0.328	0.090	0.500	0.410	52.2
	0.134	0.588	0.278	0.111	0.520	0.368	53

Table E.12 The Experimental Results for the Acetone, Methanol and Chloroform Ternary System

	Liquid Fraction			Vapour Fraction			
	Butanol	Hexene	Mek	Butanol	Hexene	Mek	Temp
Run 1	0.265	0.555	0.180	0.030	0.811	0.158	59.30
	0.268	0.558	0.175	0.021	0.826	0.152	59.40
	0.315	0.508	0.177	0.022	0.825	0.154	59.85
	0.367	0.453	0.180	0.028	0.814	0.158	60.30
	0.411	0.407	0.181	0.034	0.803	0.163	60.70
	0.459	0.360	0.181	0.041	0.749	0.210	61.55
	0.512	0.307	0.180	0.045	0.777	0.178	62.30
	0.555	0.268	0.178	0.045	0.769	0.186	63.00
Run 2	0.099	0.266	0.635	0.000	0.562	0.438	62.50
	0.099	0.248	0.653	0.000	0.551	0.449	62.90
	0.117	0.228	0.655	0.001	0.536	0.463	63.40
	0.125	0.205	0.670	0.002	0.515	0.483	64.15
	0.133	0.181	0.686	0.002	0.495	0.503	64.80
	0.156	0.154	0.691	0.004	0.463	0.533	65.50
	0.167	0.129	0.703	0.006	0.437	0.557	66.50
	0.197	0.105	0.698	0.010	0.390	0.599	67.50
	0.212	0.087	0.701	0.010	0.355	0.635	68.20
	0.248	0.057	0.695	0.027	0.279	0.695	70.45

Table E.13 The Experimental Results for the Butanol, 1-Hexene and Methyl Ethyl Ketone Ternary System

	Liquid Fraction			Vapour Fraction			
	Butanol	Hexene	Mek	Butanol	Hexene	Mek	Temp
Run 3	0.040	0.524	0.436	0.004	0.718	0.278	60.30
	0.181	0.417	0.402	0.008	0.705	0.288	60.90
	0.229	0.362	0.409	0.012	0.684	0.304	61.30
	0.261	0.322	0.417	0.012	0.673	0.314	61.65
	0.290	0.283	0.426	0.016	0.654	0.330	62.30
	0.326	0.247	0.427	0.019	0.638	0.343	62.80
	0.366	0.214	0.420	0.031	0.611	0.358	63.10
Run 4	0.156	0.750	0.094	0.014	0.894	0.092	58.40
	0.187	0.722	0.091	0.020	0.890	0.089	59.00
	0.240	0.669	0.092	0.025	0.885	0.090	59.15
	0.293	0.613	0.093	0.028	0.882	0.090	59.50
	0.379	0.526	0.094	0.035	0.874	0.092	60.20
	0.489	0.416	0.095	0.043	0.859	0.098	60.80

Table E.14 The Experimental Results for the Butanol, 1-Hexene and Methyl Ethyl Ketone Ternary System

	Liquid Fraction			Vapour Fraction			
	Butanol	Hexene	Mek	Butanol	Hexene	Mek	Temp
Run 1	0.255	0.745	0.000	0.020	0.980	0.000	60.05
	0.321	0.679	0.000	0.025	0.975	0.000	60.25
	0.394	0.606	0.000	0.026	0.974	0.000	60.50
	0.475	0.525	0.000	0.030	0.970	0.000	61.00
	0.552	0.448	0.000	0.033	0.967	0.000	61.65
	0.609	0.391	0.000	0.033	0.967	0.000	62.00
	0.663	0.337	0.000	0.040	0.960	0.000	62.90
Run 2	0.673	0.327	0.000	0.030	0.970	0.000	64.95
	0.709	0.291	0.000	0.040	0.960	0.000	65.75
	0.749	0.251	0.000	0.048	0.952	0.000	66.95
	0.776	0.224	0.000	0.052	0.948	0.000	68.05
	0.794	0.206	0.000	0.056	0.944	0.000	68.95
	0.811	0.189	0.000	0.062	0.938	0.000	70.50
	0.830	0.170	0.000	0.066	0.934	0.000	71.25
	0.845	0.155	0.000	0.076	0.924	0.000	72.80
	0.869	0.131	0.000	0.086	0.914	0.000	75.00
	0.895	0.105	0.000	0.103	0.897	0.000	77.90
	0.951	0.049	0.000	0.220	0.780	0.000	90.00

Table E.15 The Experimental Results for the Butanol and 1-Hexene Binary System

	Liquid Fraction			Vapour Fraction			
	Butanol	Hexene	Mek	Butanol	Hexene	Mek	Temp
Run 1	0.211	0.000	0.789	0.000	0.000	1.000	78.25
	0.241	0.000	0.759	0.003	0.000	0.997	78.40
	0.245	0.000	0.755	0.010	0.000	0.990	78.40
	0.255	0.000	0.745	0.0?1	0.000	0.979	78.40
	0.271	0.000	0.729	??	0.000	0.966	78.50
	0.282	0.000	0.718	?	0.000	0.961	78.75
	0.303	0.000	0.697	0.051	0.000	0.949	79.15
	0.328	0.000	0.672	0.062	0.000	0.938	79.25
	0.346	0.000	0.654	0.061	0.000	0.939	79.75
	0.390	0.000	0.610	0.079	0.000	0.921	80.40
Run 2	0.599	0.000	0.401	0.185	0.000	0.815	86.35
	0.631	0.000	0.369	0.204	0.000	0.796	86.90
	0.653	0.000	0.347	0.216	0.000	0.784	87.50
	0.673	0.000	0.327	0.225	0.000	0.775	88.00
	0.687	0.000	0.313	0.232	0.000	0.768	88.30
	0.701	0.000	0.299	0.238	0.000	0.762	88.80
	0.718	0.000	0.282	0.256	0.000	0.744	89.50
	0.734	0.000	0.266	0.267	0.000	0.733	90.00
	0.767	0.000	0.233	0.314	0.000	0.686	91.50
	0.794	0.000	0.206	0.340	0.000	0.660	92.40
	0.831	0.000	0.169	0.400	0.000	0.600	94.60

Table E.16 The Experimental Results for the Butanol and Methyl Ethyl Ketone Binary System

	Liquid Frac			Vap Frac			
	Acetone	Hexene	Mek	Acetone	Hexene	Mek	Temp
Run 1	0.451	0.445	0.104	0.504	0.453	0.043	47.40
	0.419	0.451	0.130	0.498	0.458	0.044	47.70
	0.401	0.452	0.147	0.482	0.466	0.052	48.15
	0.380	0.450	0.170	0.468	0.472	0.061	48.40
	0.358	0.444	0.198	0.466	0.474	0.060	48.75
	0.334	0.434	0.232	0.455	0.479	0.066	49.40
Run 2	0.270	0.492	0.238	0.436	0.503	0.061	50.30
	0.259	0.493	0.248	0.412	0.513	0.076	50.65
	0.245	0.490	0.265	0.364	0.527	0.109	51.30
	0.227	0.482	0.290	0.365	0.529	0.106	51.80
	0.208	0.479	0.313	0.361	0.535	0.104	51.90
	0.192	0.470	0.333	0.374	0.534	0.092	52.30
	0.181	0.463	0.356	0.385	0.529	0.086	52.70
	0.160	0.453	0.387	0.291	0.553	0.157	53.35
	0.142	0.429	0.429	0.248	0.556	0.196	54.20
Run 3	0.310	0.622	0.068	0.522	0.469	0.009	47.00
	0.297	0.632	0.071	0.521	0.469	0.010	47.25
	0.280	0.643	0.077	0.505	0.479	0.016	47.65
	0.259	0.660	0.081	0.093	0.904	0.003	47.95
	0.226	0.685	0.090	0.477	0.501	0.022	48.75
	0.196	0.707	0.097	0.485	0.495	0.020	49.00
	0.152	0.739	0.108	0.426	0.538	0.035	50.35
	0.120	0.760	0.120	0.477	0.499	0.023	50.90

Table E.17 The Experimental Data for the Acetone, Hexene and Methyl Ethyl Ketone Ternary System

	Liquid Fraction			Vapour Fraction			
	Acetone	Hexene	Mek	Acetone	Hexene	Mek	Temp
Run 4	0.034	0.805	0.161	0.258	0.647	0.095	53.75
	0.031	0.801	0.168	0.207	0.684	0.109	54.15
	0.024	0.802	0.174	0.166	0.710	0.124	54.60
	0.012	0.812	0.175	0.076	0.769	0.155	55.50
	0.006	0.814	0.181	0.051	0.785	0.164	55.50
	0.001	0.817	0.182	0.033	0.797	0.170	55.40
Run 5	0.519	0.094	0.387	0.605	0.270	0.124	54.30
	0.509	0.087	0.405	0.607	0.247	0.146	54.70
	0.500	0.082	0.418	0.607	0.233	0.159	54.90
	0.498	0.078	0.423	0.613	0.229	0.157	55.10
	0.494	0.074	0.432	0.615	0.235	0.151	55.35
	0.483	0.066	0.451	0.618	0.207	0.175	56.30
	0.471	0.056	0.473	0.623	0.189	0.187	56.80
	0.466	0.052	0.482	0.629	0.188	0.183	57.15
	0.457	0.048	0.495	0.619	0.157	0.224	57.40
	0.441	0.039	0.521	0.626	0.143	0.232	58.75
Run6	0.838	0.108	0.055	0.754	0.230	0.016	47.75
	0.845	0.097	0.058	0.765	0.217	0.018	48.10
	0.851	0.088	0.061	0.777	0.204	0.019	48.35
	0.856	0.079	0.065	0.789	0.190	0.021	48.40
	0.860	0.071	0.069	0.800	0.177	0.023	48.50
	0.869	0.055	0.076	0.829	0.144	0.027	49.50
	0.872	0.041	0.087	0.854	0.117	0.029	49.85

Table E.18 The Experimental Data for the Acetone, 1-Hexene and Methyl Ethyl Ketone Ternary System

	Liquid Fraction			Vapour Fraction			
	Acetone	Hexene	Mek	Acetone	Hexene	Mek	Temp
Run 1	0.887	0.113	0.000	0.777	0.223	0.000	47.25
	0.907	0.093	0.000	0.798	0.202	0.000	47.65
	0.918	0.082	0.000	0.808	0.192	0.000	47.65
	0.929	0.071	0.000	0.824	0.176	0.000	47.70
	0.939	0.061	0.000	0.836	0.164	0.000	47.60
	0.954	0.046	0.000	0.876	0.124	0.000	48.45
	0.971	0.029	0.000	0.907	0.093	0.000	48.80
Run 2	0.582	0.418	0.000	0.579	0.421	0.000	44.95
	0.568	0.432	0.000	0.577	0.423	0.000	44.70
	0.563	0.437	0.000	0.576	0.424	0.000	44.60

Table E.19 The Experimental Results for the Acetone and 1-Hexene Binary System

	Liquid Fraction			Vapour Fraction			
	Acetone	Hexene	Mek	Acetone	Hexene	Mek	Temp
Run 1	0.558	0.000	0.442	0.962	0.000	0.038	57.90
	0.559	0.000	0.441	0.902	0.000	0.098	58.40
	0.554	0.000	0.446	0.875	0.000	0.125	58.50
	0.540	0.000	0.460	0.863	0.000	0.137	58.90
	0.513	0.000	0.487	0.846	0.000	0.154	59.55
	0.490	0.000	0.510	0.870	0.000	0.130	60.10
	0.470	0.000	0.530	0.831	0.000	0.169	60.70
Run 2	0.334	0.000	0.666	0.886	0.000	0.114	64.00
	0.315	0.000	0.685	0.862	0.000	0.138	64.20
	0.305	0.000	0.695	0.888	0.000	0.112	64.50
	0.296	0.000	0.704	0.911	0.000	0.089	64.70
	0.277	0.000	0.723	0.835	0.000	0.165	65.20
	0.242	0.000	0.758	0.615	0.000	0.385	66.80
	0.203	0.000	0.797	0.655	0.000	0.345	67.50
	0.180	0.000	0.820	0.712	0.000	0.288	68.10
	0.159	0.000	0.841	0.731	0.000	0.269	68.60

Table E.20 The Experimental Results for the Acetone and Methyl Ethyl Ketone Binary System

Liquid Fraction			Vapour Fraction			
Acetone	Hexene	Mek	Acetone	Hexene	Mek	Temp
0.000	0.804	0.196	0.000	0.822	0.178	56.20
0.000	0.808	0.192	0.000	0.809	0.191	56.25
0.000	0.806	0.194	0.000	0.807	0.193	56.25
0.000	0.805	0.195	0.000	0.806	0.194	56.40
0.000	0.798	0.202	0.000	0.801	0.199	56.45
0.000	0.794	0.206	0.000	0.799	0.201	56.05
0.000	0.788	0.212	0.000	0.792	0.208	55.90
0.000	0.522	0.478	0.000	0.679	0.321	58.00
0.000	0.519	0.481	0.000	0.689	0.311	58.00
0.000	0.509	0.491	0.000	0.679	0.321	58.15
0.000	0.500	0.500	0.000	0.679	0.321	58.20
0.000	0.489	0.511	0.000	0.674	0.326	58.45
0.000	0.475	0.525	0.000	0.665	0.335	58.50
0.000	0.459	0.541	0.000	0.665	0.335	58.50
0.000	0.429	0.571	0.000	0.633	0.367	59.40
0.000	0.388	0.612	0.000	0.623	0.377	59.40
0.000	0.346	0.654	0.000	0.609	0.391	59.60
0.000	0.303	0.697	0.000	0.571	0.429	60.90

Run 1 corresponds to the first seven data rows, and Run 2 corresponds to the remaining data rows.

Table E.21 The Experimental Results for the 1-Hexene and Methyl Ethyl Ketone Binary System

	Liquid Fraction			Vapour Fraction			
	Acetone	Hexene	Mek	Acetone	Hexene	Mek	Temp
Run 3	0.000	0.922	0.078	0.000	0.870	0.130	56.80
	0.000	0.932	0.068	0.000	0.889	0.111	56.90
	0.000	0.941	0.059	0.000	0.901	0.099	56.85
	0.000	0.942	0.058	0.000	0.905	0.095	56.85
	0.000	0.947	0.053	0.000	0.909	0.091	56.85
	0.000	0.954	0.046	0.000	0.911	0.089	56.75
	0.000	0.957	0.043	0.000	0.910	0.090	56.60
	0.000	0.961	0.039	0.000	0.926	0.074	56.80

Table E.22 The Experimental Results for the 1-Hexene and Methyl Ethyl Ketone Binary System

Author: Chronis Theodoros.
Name of thesis: The simple measurement of residue curves and the associated VLE data for ternary liquid mixtures.

PUBLISHER:
University of the Witwatersrand, Johannesburg
©2015

LEGALNOTICES: